



# Formation and evolution of an Early Cambrian foreland basin in the NW Yangtze Block, South China

Zhidong Gu<sup>1\*</sup>, Xing Jian<sup>2</sup>, Anthony B. Watts<sup>3</sup>, Xiufen Zhai<sup>1</sup>, Guixia Liu<sup>1</sup> and Hua Jiang<sup>1</sup>

<sup>1</sup> Research Institute of Petroleum Exploration and Development (RIPED), PetroChina, Beijing 100083, China

<sup>2</sup> State Key Laboratory of Marine Environmental Science, College of Ocean and Earth Sciences, Xiamen University, Xiamen 361102, China

<sup>3</sup> Department of Earth Sciences, Oxford University, Oxford OX1 3AN, UK

ZG, 0000-0002-3529-4198

\* Correspondence: [guzhidong@petrochina.com.cn](mailto:guzhidong@petrochina.com.cn)

**Abstract:** The Ediacaran to Cambrian succession in the NW Yangtze Block has long been considered to have formed in a passive margin. The Ediacaran is dominated by thick carbonate rocks, whereas the Lower Cambrian comprises a thick clastic succession. The transition from carbonate to clastic rocks and the provenance and tectonic setting of the clastic succession are poorly understood. Stratigraphic correlation shows a distinct stratigraphic absence from the Lower Cambrian to Devonian in the Bikou terrane. A regional seismic profile shows a wedge geometry of the Lower Cambrian from NW to SE. Outcrops reveal an overall coarsening-upward Lower Cambrian succession. The petrographic analysis of clastic rocks indicates immaturity, implying a proximal source. Palaeocurrent measurements of clastic rocks point to dominant SE-vergent orientations. The age spectra of detrital zircons imply that they were derived from Early Cambrian continental arcs and older continental crust. Geological, geophysical and geochemical evidence indicates that an Early Cambrian foreland basin was formed in the NW Yangtze Block. This foreland basin appears to have been strongly influenced by orogenic loading northwestward. We propose that this orogenic event should be named the Motianling orogeny, the origin of which may be related to subduction of the Proto-Tethys ocean beneath the NW Yangtze Block.

**Supplementary material:** Supplementary tables A–D and a petrological description of detrital zircons are available at <https://doi.org/10.6084/m9.figshare.c.6332980>

Received 22 August 2022; revised 30 October 2022; accepted 27 November 2022

The formation of a foreland basin is generally related to building of an orogen on a passive margin and resulting lithospheric flexure on a craton (Speed and Sleep 1982; Cant and Stockmal 1989; Ettensohn 1993). Furthermore, the initiation of a foreland basin is commonly followed by a tectonic transition from a passive margin to oceanic plate subduction and subsequent collision of the passive margin with island or continental arcs or microterranes (Dewey 1969b, 1971; Jacobi 1981; Cohen 1982; Read 1982; Gutschick and Sandberg 1983; Thomas 1983; Walker *et al.* 1983; Bradley and Kusky 1986; Houseknecht 1986; Stockmal *et al.* 1986; Robertson 1987a, b; Pigram *et al.* 1989; Karabinos *et al.* 1998; Bradley 2008; Read and Repetski 2012). Tectonic transitions from a passive margin to a foreland basin have been documented and studied in many orogens in the world, and of these the Appalachian orogen (Bird and Dewey 1970; Hiscott 1978; Read 1980; Cooper *et al.* 2001; Read and Repetski 2012; Sinha *et al.* 2012; Gbadeyan and Dix 2013) and the Caledonian orogeny (Dewey 1969a, 1971; Dewey and Mange 1999; McKerrow *et al.* 2000; Wickstrom and Stephens 2020) were the earliest and most thoroughly studied examples, which provide essential models for the transition.

The Ediacaran to Cambrian succession in the NW Yangtze Block, South China, has long been considered to have formed in a passive margin setting (Zhang *et al.* 1995; Liu and Zhang 1999; Meng and Zhang 1999; Dong *et al.* 2015; Chen *et al.* 2016, 2018; Dong and Santosh 2016; Domeier 2018; Yan *et al.* 2018b), and the Cambrian clastic rocks were thought to be derived from the Cathaysia Block to the SE (Wang *et al.* 2010) or from the exotic blocks located along the northwestern margin of East Gondwana (Yao *et al.* 2014; Chen *et al.* 2016). Gu *et al.* (2016a) found that a succession consisting dominantly of a thick wedge of Lower

Cambrian clastic rocks occurred in the NW Sichuan Basin overlapping from NW to SE. However, the provenance and tectonic setting of the Lower Cambrian clastic rocks remain poorly known.

The aims of this study are to analyse the provenance and depositional process of the Lower Cambrian clastic rocks, and to test the occurrence of an early Cambrian foreland basin, as well as further to analyse its formation and evolution. This paper provides insights into the tectonics and geodynamics of the NW Yangtze Block as well as the restoration of East Gondwana, and is expected to have significant implications for the Lower Cambrian gas exploration of the Sichuan Basin.

## Geological setting

### Regional tectonic setting

The South China Craton consists of the Yangtze Block to the NW and the Cathaysia Block to the SE, which were assembled along the Jiangnan orogen at *c.* 820 Ma during the early Neoproterozoic (Zhao and Cawood 2012; Domeier 2018). Following the assembly, the South China Craton experienced continental rifting along the Jiangnan orogen at *c.* 820–750 Ma, which formed the Nanhua rift basin, and along the western Yangtze Block, which formed the Kangdian rift basin (Wang and Li 2003; Li *et al.* 2013; Domeier 2018). These rift basins failed and did not evolve into oceanic basins, resulting in the formation of intracontinental failed rifts during the Neoproterozoic (Charvet *et al.* 2010; Li *et al.* 2010; Domeier 2018). These failed rifts could play crucial roles in the deposition of the Ediacaran to Middle Ordovician succession as a result of thermal subsidence produced by rifting (Gu *et al.* 2021).

During the Late Ordovician to Silurian, the southeastern Yangtze Block was developed in a foreland basin related to the flexural influence of the Kwangsi orogeny occurring in the Cathaysia Block (Li *et al.* 2013; Domeier 2018); the NW Yangtze Block was also affected by a contemporaneous tectonic event resulting in the formation of an approximately east–west uplift (referred to as the Leshan–Longnüsi uplift by previous studies) in the central and western Sichuan Basin (Song 1987, 1996), although the dynamics of the uplift remains unclear.

The Sichuan Basin is located in the NW Yangtze Block. The tectonic units from the Sichuan Basin northwestward are successively the Longmenshan fold–thrust belt, the Songpan–Ganzi terrane, the Bikou terrane, the Qinling orogen and the North China Craton (Figs 1 and 2) (Dong and Santosh 2016; Ye *et al.* 2017; Li *et al.* 2018). The NE-trending Longmenshan fold–thrust belt has a c. 500 km length from NE to SW and 50 km width from SE to NW, and is separated from the Sichuan Basin by the Guanxian–Anxian fault in the SE, from the Bikou terrane by the Pingwu–Qingchuan fault in the NW, and from the Songpan–Ganzi terrane by the Wenchuan–Maoxian fault in the west (Chen and Wilson 1996; Jia *et al.* 2006; Li *et al.* 2012; Xue *et al.* 2017; Yan *et al.* 2018b) (Figs 1 and 2). The Longmenshan fold–thrust belt experienced at least two tectonic events: one that occurred during the convergence between the Yangtze Block and Songpan–Ganzi terrane in the Late Triassic and another that resulted from the convergence between the Tibetan Plateau and the Sichuan Basin in the Cenozoic (Li *et al.* 2003; Wang *et al.* 2014; Yan *et al.* 2018a).

The Bikou terrane is separated from the West Qinling orogen by the Mianlue suture in the NW (Meng and Zhang 1999; Dong *et al.* 2015; Hui *et al.* 2020) (Figs 1 and 2). The Archean Yudongzi Group and the Paleoproterozoic Hejiayan Group are restricted to the NE of the terrane (Yan *et al.* 2018b; Hui *et al.* 2021). The terrane is mainly composed of a lower greenschist-facies metamorphic complex of

Neoproterozoic age, consisting of the Bikou Group volcanic succession in the SE and the Hengdan Group volcanoclastic turbidite succession in the NW, which are separated by the Fengxiangyuan–Tongqianba fault (Druschke *et al.* 2006; Wang *et al.* 2008; Dong and Santosh 2016; Gao *et al.* 2020; Hui *et al.* 2020) (Figs 1 and 2). The Cryogenian Guanjiagou Formation, located in the NW of the terrane, unconformably overlies the Hengdan Group, representing Neoproterozoic diamictite-bearing glacial deposits (Mao *et al.* 2021). It is overlain by Ediacaran–Lower Cambrian slope-basin facies carbonates, siliciclastic rocks and cherts, which are generally unconformably overlain by Devonian units.

The triangular Songpan–Ganzi terrane is a tectonic junction between the South China Craton, the North China Craton and Central Tibet (Zhang *et al.* 2006) (Fig. 1). It is proposed that the basement of the Songpan–Ganzi terrane is a remnant oceanic basin (Palaeo-Tethys) (Zhou and Graham 1996) or has an affinity with the Yangtze Block (Zhang *et al.* 2006; Chang 2010). The sediments of the terrane are mainly composed of a thick (c. 5–15 km) marine Triassic flysch turbidite succession, which subsequently experienced low-grade greenschist-facies metamorphism and was intensively folded during the Late Triassic Indosinian orogeny (Chen *et al.* 1995; Zhang *et al.* 2006; Li *et al.* 2012; Xue *et al.* 2017).

The west–east-trending Qinling orogen in central China is the product of the Late Triassic collision between the North and South China cratons along the Mianlue suture (Mattauer *et al.* 1985; Zhang *et al.* 1995; Meng and Zhang 1999; Zheng *et al.* 2010; Dong *et al.* 2015). The Qinling orogen, from west to east, can be divided into the West Qinling and East Qinling orogens (Zhang *et al.* 1995, 1996; Zheng *et al.* 2010; Li *et al.* 2018) (Fig. 1); the East Qinling orogen is further subdivided into the North Qinling and South Qinling orogens, separated by the Early Paleozoic Sangdan suture (Meng and Zhang 1999; Zheng *et al.* 2010; Dong *et al.* 2015, 2017) (Fig. 1). The South Qinling orogen has long been considered as the passive

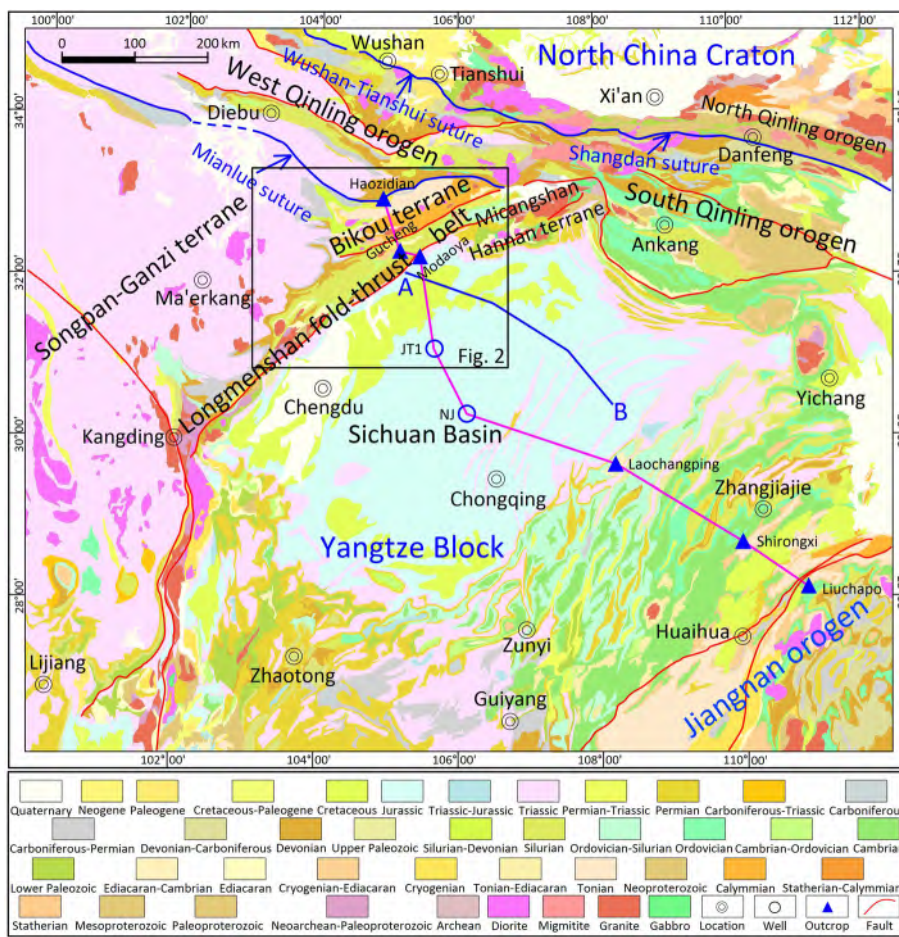


**Fig. 1.** Overview geological map of the NW Yangtze Block (modified after the 1:2 500 000 geological map by Ye *et al.* 2017), showing the tectonic units and the locations of the seismic reflection profile A–B and lithostratigraphic correlation (pink line). The map also shows the Triassic boundary of the Yangtze Block and North China Craton (i.e. the Mianlue suture), and the Ediacaran–Cambrian boundary of the Yangtze Block and North China Craton (i.e. the Wushan–Tianshui and Shangdan sutures). The black box indicates the main area of this study as shown in Figure 2. Quat, Quaternary; Neog, Neogene; Palg, Paleogene; Cret, Cretaceous; Jura, Jurassic; Tria, Triassic; Perm, Permian; Carb, Carboniferous; Devo, Devonian; Up-Palz, Upper Paleozoic; Silu, Silurian; Ordo, Ordovician; Camb, Cambrian; Lo-Palz, Lower Paleozoic; Edia, Ediacaran; Cryo, Cryogenian; Toni, Tonian; Neop, Neoproterozoic; Caly, Calymnian; Stat, Statherian; Mesp, Mesoproterozoic; Palp, Paleoproterozoic; Arch, Archean; Neoa, Neoproterozoic; Dior, Diorite; Migm, Migmatite; Gran, Granite; Gabb, Gabbro.

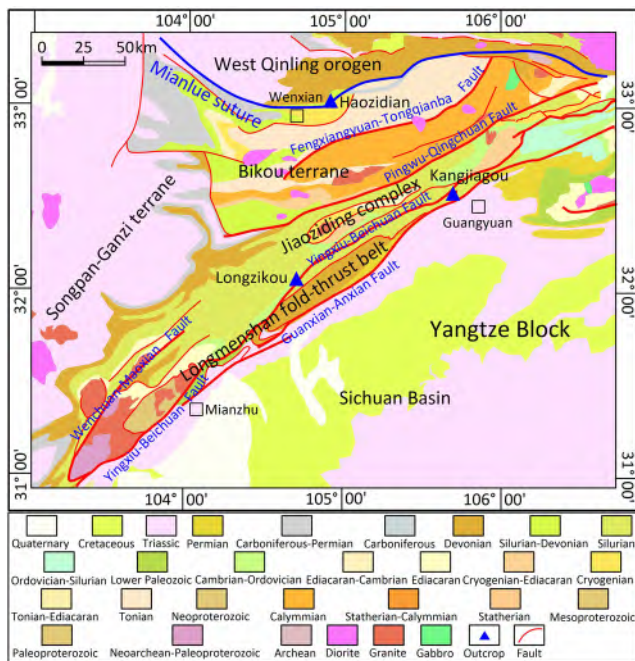


**Fig. 2.** Simplified geological map of the NW Yangtze Block, showing details of the tectonic units in Figure 1 and locations of representative outcrop sections within the Longmenshan fold–thrust belt.

margin of the Yangtze Block during the Late Neoproterozoic to Early Paleozoic (Zhang *et al.* 1995; Meng and Zhang 1999; Zheng *et al.* 2010; Dong *et al.* 2015, 2017; Dong and Santosh 2016). The West Qinling orogen is a western extension of the South Qinling orogen, which is bounded by the Wushan–Tianshui suture in the north and Mianlue suture in the south (Pei *et al.* 2004; Li *et al.* 2018; Yang *et al.* 2018). The Wushan–Tianshui suture is considered as the westward extension of the Sangdan suture and comprises ophiolite complexes and island-arc units (Pei *et al.* 2004, 2007a, b, c, 2009; Dong *et al.* 2007; Li *et al.* 2007; Yang *et al.* 2018).

### Stratigraphy of the Cambrian

For the West Qinling orogen, only the Lower Cambrian exists at Baiyigou in Ruergai County in the most southerly orogen (Fig. 1), and is referred to as the Taiyangding Group (*c.* 800–1000 m thick) (Ye *et al.* 1994; Liu *et al.* 2004). The Taiyangding Group unconformably overlies the Cryogenian Baiyigou Group, which is dominated by volcanoclastic rocks and terrestrial clastic rocks that may reveal the absence of the Ediacaran, and is in faulted contact with the Middle–Late Ordovician (Liu *et al.* 2004). It is mainly composed of a thick sequence of cherts (more than 500 m thick) and thin slates with minor siliciclastic rocks and carbonates (Jiang 1994; Liu *et al.* 1998, 2004).

In the Bikou terrane, only the Lower Cambrian occurs in the NW of the terrane, and is referred to as the Gangou Formation. It conformably overlies the Ediacaran Dengying Formation, and is unconformably overlain by Lower–Middle Devonian units. The Gangou Formation (*c.* 70–530 m thick) mainly consists of thick black cherts interbedded with thin banded limestones and phosphorite nodules in the lower part, and black carbonaceous shales with cherts and thin limestones in the upper part, and is constrained by the presence of Early Cambrian fossils, such as small shelly fossils, hyoliths and sponge spicules in the shales and limestones (Qin *et al.* 1990; Zhao *et al.* 1990; Li 1991).

In the Longmenshan fold–thrust belt, more stratigraphic units of the Cambrian occur than in the above tectonic units; from base to top these consist of the Maidiping, Qiongzhusi and Canglangpu formations. The Maidiping Formation is mainly composed of interbedded thin chert and phosphoric carbonate, and thin black

shale (Gu *et al.* 2021). The Qiongzhusi Formation is defined by the first occurrence of trilobites, and consists of organic-rich black shale that gradually coarsens upward into muddy siltstones and siltstones (Gu *et al.* 2021). Above the Qiongzhusi Formation, the Canglangpu Formation consists of coarsening-upward medium to thick siltstones, sandstones and conglomerates. The Canglangpu Formation is generally unconformably overlain by Ordovician, Silurian or Devonian rocks in the Longmenshan region.

In the Sichuan Basin, there are many wells penetrating the Cambrian. Generally, the Lower Cambrian in the west is more complete than that in the east, whereas the Middle–Upper Cambrian in the west is less complete than that in the east. Above the Canglangpu Formation, the Longwangmiao Formation consists mainly of dolomitized limestones, with lesser amounts of argillaceous and sandy dolomites and a thin interval of siliciclastic rocks in the middle of the succession (Gu *et al.* 2021). The overlying Douposi Formation of the Middle Cambrian consists of mixed siliciclastic rocks, carbonates and evaporites, deposited in shallow water environments. The Xixiangchi Formation of the Middle–Upper Cambrian consists mainly of medium to thick carbonates deposited in a shallow water environment.

### Data, samples and methods

#### Data

To decipher the Cambrian tectonosedimentary evolution in the NW Yangtze Block, we integrated seismic and well data in the Sichuan Basin with field outcrops within the Longmenshan fold–thrust belt. We constructed a NW–SE lithostratigraphic correlation section across the Yangtze Block combining outcrops and well data to show the distribution and variation of the Cambrian rocks. We carefully chose and measured the Longzikou section in Beichuan County and the Kangjiagou section in Guangyuan City, which are located in the Longmenshan fold–thrust belt (Fig. 2). In terms of seismic data, we constructed an approximately 400 km long regional cross-section by using some representative 2D and 3D lines to reveal the structure of the Sichuan Basin.

#### Samples

We chose mainly two representative sections (*i.e.* the Longzikou and Kangjiagou sections; Fig. 2) for systematic collection of samples to reveal sedimentary and tectonic variations. We collected 48 shale samples and 41 siltstone to sandstone samples from the Longzikou section for analysing the major and trace elements, 21 medium- to coarse-grained sandstone samples from the Kangjiagou section for framework grain petrography and heavy mineral analyses and six sandstone samples from the Longzikou (three samples) and Kangjiagou (three samples) sections for detrital zircon U–Pb–Hf isotopic analyses.

#### Methods

##### Whole-rock major, trace and rare earth element analyses

Whole-rock major and trace elemental compositions were analysed at the Analytical Laboratory, Beijing Research Institute of Uranium Geology. Samples were crushed and powered to less than 200 mesh for elemental analyses. The loss on ignition (LOI) values were obtained by measuring the weight loss after heating the sample powders at 980°C. Whole-rock major element analyses were measured by X-ray fluorescence spectrometry (XRF) using an Axios-mAX system. Trace elements (REE included) were analysed by inductively coupled plasma mass spectrometry (ICP-MS) using an Element XR system. Both precision and accuracy were better than 5 and 10% for major and trace elements, respectively.

### Framework grain petrography

Sandstone samples were polished into standard thin sections for petrography study. The sandstone thin sections were then observed under a polarizing microscope. Framework grains, including quartz, plagioclase, K-feldspar and various lithic fragments, were identified and sedimentary textures, such as grain size, sorting and roundness, were observed and analysed. Twenty-one Canglangpu Formation sandstone samples from the Kangjiagou section were selected for modal analysis by using the Gazzi–Dickinson method (Dickinson 1985). More than 400 points were counted per thin section.

### Heavy mineral analyses

The procedures for heavy mineral analyses have been given by Jian *et al.* (2013, 2020). Fresh sandstone samples were first simply crushed and then 63–250  $\mu\text{m}$  fractions were separated with sieves. To remove carbonate minerals, the 63–250  $\mu\text{m}$  fraction grains were soaked in 1N acetic acid for 24 h at 60°C. Heavy minerals were then separated from the carbonate-free 63–250  $\mu\text{m}$  fractions using the heavy liquid tribromomethane (2.89 g  $\text{cm}^{-3}$ ) and mounted on glass slides with Canada balsam. About 200 transparent heavy mineral grains were identified and point-counted at suitable regular spacing under a polarizing microscope (Mange and Maurer 1992).

### Zircon U–Pb isotopic analyses

Zircon separation and cathodoluminescence (CL) imaging were performed using the same methods as described by Chen *et al.* (2016, 2018). Zircon grains were separated from samples by conventional density and magnetic techniques and then were carefully hand-picked under a binocular microscope. The zircon grains were mounted in epoxy resin and polished to half section to expose the internal structure of the zircon grains. All the mounted zircon grains were photographed under reflected and transmitted light, followed by CL imaging to find domains within grains for analysis. Zircon U–Pb dating was performed by laser ablation multi-collector inductively coupled plasma mass spectrometry (LA-MC-ICP-MS) at Mineral and Fluid Inclusion Microanalysis Lab, Geology Institute, Chinese Academy of Geological Sciences, Beijing. The detailed analytical methods have been described by Zhang *et al.* (2019). Common-Pb correction followed the method of Andersen (2002). Analysis results are presented with 2 $\sigma$  error and in concordia diagrams.  $^{207}\text{Pb}/^{206}\text{Pb}$  age is used as a more precise result for zircons older than 1000 Ma, whereas  $^{206}\text{Pb}/^{238}\text{U}$  age is used for zircons younger than 1000 Ma (Chen *et al.* 2016). Age calculation and concordia diagrams were made using ISOPLOT 3.0 (Ludwig 2003).

### Lu–Hf isotopic analyses

Zircon grains with measured concordant U–Pb ages (<10% discordance) were selected for Lu–Hf isotopic measurement. The analyses were conducted at the Mineral Laser Microprobe Analysis Laboratory (Milma Lab), China University of Geosciences, Beijing (CUGB) by MC-ICP-MS, using a Thermo-Finnigan Neptune Plus and a Geolas 193 ns ArF excimer laser ablation system. During the analyses, the  $^{176}\text{Hf}/^{177}\text{Hf}$  ratio of standard zircon Mud Tank was determined to be  $0.282513 \pm 23$  (2SD,  $n = 40$ ), within error of the recommended  $^{176}\text{Hf}/^{177}\text{Hf}$  ratio of  $0.282507 \pm 6$  (2SD,  $n = 5$ ) as described by Zhang *et al.* (2019). To calculate initial  $^{176}\text{Hf}/^{177}\text{Hf}$  ratios, we used the measured  $^{176}\text{Lu}/^{177}\text{Hf}$  ratios and the  $^{176}\text{Lu}$  decay constant of  $1.867 \times 10^{-11} \text{ a}^{-1}$  (Soderlund *et al.* 2004). Moreover, calculation of  $\varepsilon_{\text{Hf}}(t)$  was based on the chondritic values of  $^{176}\text{Hf}/^{177}\text{Hf}$  (0.282772) and  $^{176}\text{Lu}/^{177}\text{Hf}$  (0.0332) reported by Blichert-Toft and Albarède (1997). To calculate depleted-mantle model ages ( $T_{\text{DM}}$ ), we took present-day  $^{176}\text{Hf}/^{177}\text{Hf} = 0.28323$ , and assumed an initial value of  $^{176}\text{Hf}/^{177}\text{Hf} = 0.27982$ , as well as  $^{176}\text{Lu}/^{177}\text{Hf} = 0.0384$  (Belousova *et al.* 2010). The crustal model

ages ( $T_{\text{DM}2}$ ) were calculated assuming that the zircon's parental magma was produced from an average continental crust ( $^{176}\text{Lu}/^{177}\text{Hf} = 0.015$ ; Griffin *et al.* 2004) that was originally derived from the depleted mantle (Belousova *et al.* 2010).

## Results

### Stratigraphic correlation

Spatial distribution and correlation of sedimentary strata can effectively help to identify tectonic events in deep time. In this study, we compiled a NW–SE Lower Cambrian correlation chart integrating outcrops and wells across the Yangtze Block (Fig. 3). The stratigraphic absence from the Lower Cambrian to Devonian occurs from NW to SE in the NW Yangtze Block. In the Bikou terrane, the Lower Cambrian Gangou Formation is unconformably overlain by the Devonian, with considerable strata lacking from at least the Middle Cambrian to Silurian, indicating that one or more tectonic uplift events took place during the Early Cambrian to Devonian. To the SE in the Longmenshan fold–thrust belt, the Lower Cambrian Qiongzhusi Formation is unconformably overlain by the Silurian, also indicating that one or more tectonic uplift events occurred in the region. Further to the SE at the Modaoya section within the Longmenshan fold–thrust belt, the Lower Cambrian Changlangpu Formation is unconformably overlain by the Ordovician Baota Formation, which also reveals some Cambrian tectonic events in the region. To the SE again, however, in the central and eastern Sichuan Basin, as well as in the Hunan regions, the stratigraphic absences occur from the Lower Ordovician to Devonian or Permian, and the Cambrian strata were continuously deposited. For example, in the central Sichuan Basin, the Lower Ordovician Meitan Formation, in well JT1, is unconformably overlain by Permian strata; the Nanjingguan Formation, in well NJ, is unconformably overlain by Permian strata. The stratigraphic absence in the central Sichuan Basin is a response to the orogeny during the Late Ordovician to Silurian referred to as the Caledonian orogeny by previous Chinese workers in comparison with an orogeny of approximately the same period in Europe (Song 1987, 1996). Further to the SE, the Lower Silurian Luoreping Formation, at the Laochangping section in Pengshui County of Chongqing City, is unconformably overlain by the Devonian. Further to the SE again, the Lower Silurian Shamao and Luoreping formations, at the Shirongxi section of Yongshun County and at the Liuchapo section of Anhua County, Hunan Province, are both unconformably overlain by the Devonian. The stratigraphic absences in the SE Yangtze Block are related to the Kwanghsian orogeny that occurred in the Cathaysia Block.

### Seismic interpretation

As the Ediacaran–Cambrian exploration in the Sichuan Basin proceeds, several wells have been drilled in the western basin and a large amount of seismic data has been collected across the basin. The seismic interpretation of Ediacaran–Cambrian horizons is based on well stratigraphic division and calibration from wells to seismic profiles. An appropriately 400 km regional seismic profile from NW to SE across the Sichuan Basin was constructed by integrating 2D and 3D seismic data to show the structure of the basin from the Ediacaran to Lower Cambrian (Figs 1 and 4). The seismic profile shows that the Ediacaran is thickened (*c.* 1800 m thick) in the NW with two sharp margin edges and is onlapping from NW to SE, related to the development of two periods of carbonate platform margins in the NW (Gu *et al.* 2016a, 2021). The seismic profile also shows that the Ediacaran is thinned (*c.* 250 m thick) in the SE, which is related to the development of an uplift in the eastern Sichuan Basin (Gu *et al.* 2016b). The Lower Cambrian succeeds the

structure of the underlying Ediacaran, which is onlapping from NW to SE, being thickened in the NW trough (c. 1500 m thick) and thinned in the SE uplift (c. 400 m thick).

**Outcrop sedimentological and petrological features and interpretations**

*Longzikou section in Beichuan County*

The Longzikou section is the most complete Lower Cambrian exposure, with a thickness of c. 1170 m. At this section, the Ediacaran Dengying Formation and the base of the Lower Cambrian are not exposed (Fig. 5a). Three formations (the Maidiping, Qiongzhusi and Canglangpu formations) are identified from base to top, which show an overall coarsening-upward succession (Fig. 5a). The Maidiping Formation (c. 316 m thick) is mainly composed of thick chert (c. 43 m thick), and interbedded chert and black shale (c. 37 m thick) (Figs 6a and 7a), with minor banded dolomite and chert (Fig. 6b). The occurrence of the thick chert and black shale reveals a deep-water depositional environment. The Qiongzhusi Formation (c. 210 m thick) mainly consists of black shale (Fig. 6c) interbedded with thin chert and minor volcanic ash

beds (Fig. 6d), grading into silty mudstone at the top (Fig. 7b). The Canglangpu Formation (c. 647 m thick) shows an overall coarsening-upward sequence, grading from thin limestone and argillaceous siltstone at the base (Figs 6e and 7c) to sandstone in the middle (Figs 6f, g and 7d) and coarse sandstone with minor conglomerate rocks at the top (Figs 6h and 7e, f). The compositions of the conglomerate and sand grains are varied, including different kinds of fragments such as volcanic, siliceous, siliciclastic and carbonate fragments, with some micrite envelopes and carbonate replacements or cements. The Canglangpu Formation sandstones are unconformably overlain by Ordovician limestones.

This section reveals a transition from a deep-water depositional environment to a shallow water depositional environment. The chert, siltstone and sandstone assemblage in the middle and lower part shows frequent changes in composition, and low degree of rounding (Fig. 7a–c). The sandstones and conglomerates in the upper part of this section show very poor sorting and angular shapes of detrital sediments, indicating a proximal detrital source (Fig. 7d–f). The composition of rock fragments is very complex, including chert, siliciclastic rock, carbonate rock and volcanic rock fragments. The volcanic fragments are represented by intermediate–felsic igneous rocks, revealing nearby volcanic activity. The Canglangpu

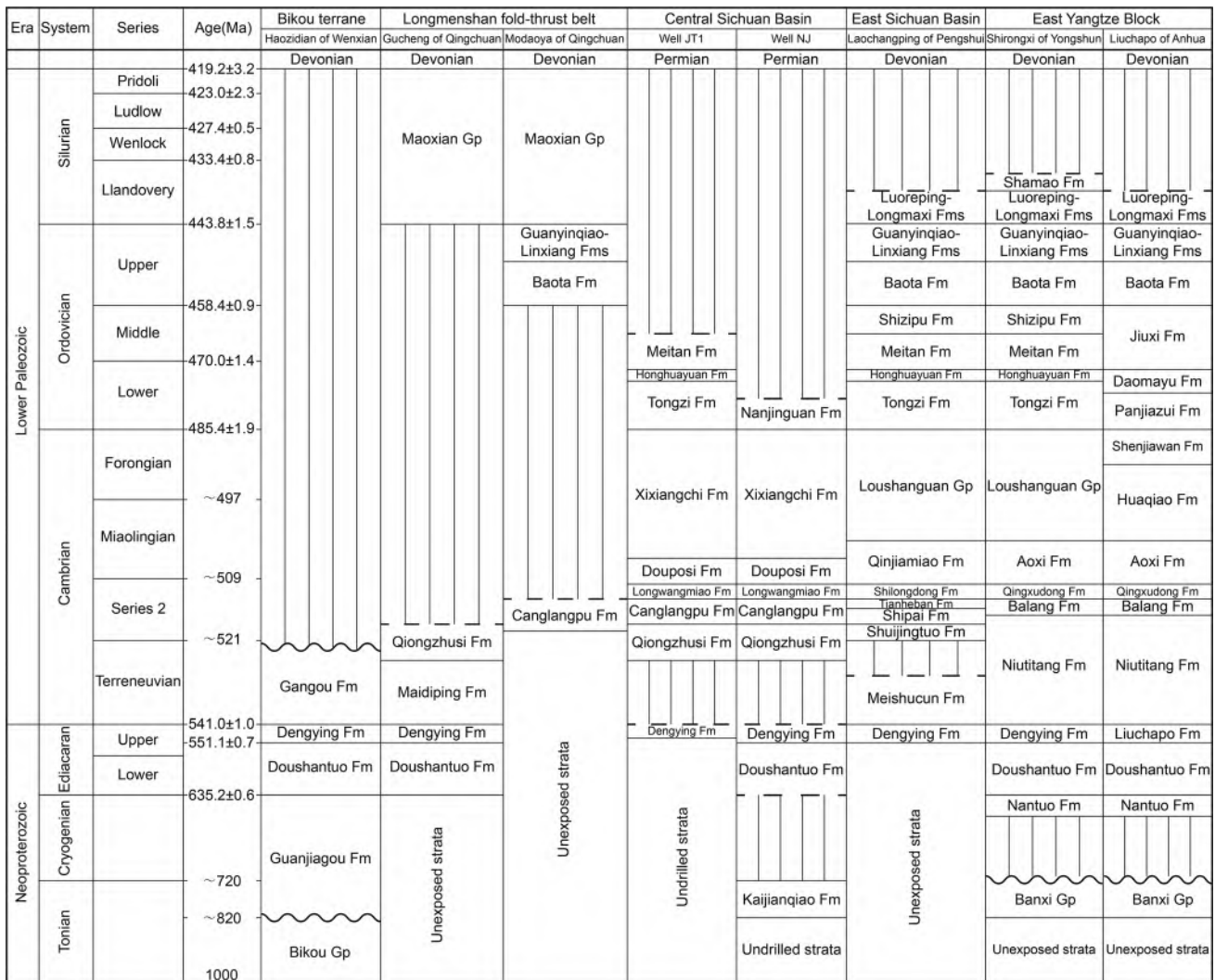


**Fig. 3.** Lithostratigraphic correlation chart for the Neoproterozoic to Lower Paleozoic across the Yangtze Block from NW to SE (compiled after field geological survey and drilling well results; radiometric ages are from International Commission on Stratigraphy, 2020, [www.stratigraphy.org](http://www.stratigraphy.org)). A considerable stratigraphic absence from the Lower Cambrian to Upper Devonian–Ordovician occurs in the Bikou terrane and the Longmenshan fold–thrust belt, revealing that one or more tectonic events took place during the Early Cambrian to Devonian. The stratigraphic absence from Ordovician to Permian in the central and eastern Sichuan Basin as well as the eastern Yangtze Block is related to the Kwangsi orogeny, which occurred in the Cathaysia Block. Gp, Group; Fm, Formation.

Formation is unconformably overlain by Ordovician rocks with considerable stratigraphic absence, from at least the Middle Cambrian to Ordovician, which reveals that an uplift event took place after the Canglangpu Formation deposition until the Ordovician. Hence, this uplift event predated the Late Ordovician to Silurian tectonic event.

#### *Kangjiagou section in Lizhou District of Guangyuan City*

The Kangjiagou section exposes the Canglangpu Formation only in the core of an anticline, with a thickness of *c.* 470 m (Fig. 5b). The section begins with a set of dolomite (*c.* 60 m thick) (Fig. 8a and b), which represents a marker horizon occurring at the base of the Canglangpu Formation in the Sichuan Basin and adjacent regions. Above the dolomite, the stratigraphic succession shows an overall coarsening-upward sequence that can be further subdivided into several cycles (Fig. 5b). In the upper part of the succession, a set of coarse-grained sandstone with conglomerate (*c.* 120 m thick) (Figs 8c, f and 9a, b) and an overlying massive conglomerate (*c.* 80 m thick) (Figs 8g, h and 9e, f) are present. The interbedded siltstones are mainly composed of very fine quartz, mica grains and carbonate cements (Fig. 9c and d). Clasts within the conglomerate contain various rock types including dominant cherts, metasedimentary rocks (e.g. greenschist and slate), granites and sedimentary rocks (e.g. mudstones and carbonates). The grains are very poorly sorted, with angular shapes, indicating a nearby detrital source (Fig. 9e and f).

The measurement results of the palaeocurrent orientations, mainly based on cross-bedding (Fig. 8c) and current ripples (Fig. 8d), indicate NW detritus sources. Based on investigation in adjacent regions, the dominant chert clasts may be derived from the Lower Cambrian or the Ediacaran Doushantuo Formation in the Bikou terrane and West Qinling orogen. Furthermore, the metasedimentary rocks, especially the greenschist, are derived from the Bikou Group in the Bikou terrane, where the greenschist is considerably developed at more than 1000 m thickness.

Therefore, the section not only shows an orogeny to the NW of the present-day Longmenshan fold–thrust belt, but also shows that the Canglangpu Formation sedimentary rocks were most probably sourced from the Bikou terrane and/or West Qinling orogen. The development of the thick conglomerate in the upper part of the succession reveals a period of intense orogeny in the NW Bikou terrane and adjacent regions. All the evidence demonstrates that an orogen formed during the Early Cambrian in the Bikou terrane and adjacent regions and a foreland basin formed in the present-day Longmenshan fold–thrust belt.

#### *Sandstone framework grain composition*

The Canglangpu Formation sandstones from the Kangjiagou section are characterized by high lithic fragment (25–85%, averaging 55%) and quartz (8–60%, averaging 37%) contents and relatively low feldspar (2–21%, averaging 8%) contents (Figs 9 and 10a). Feldspar

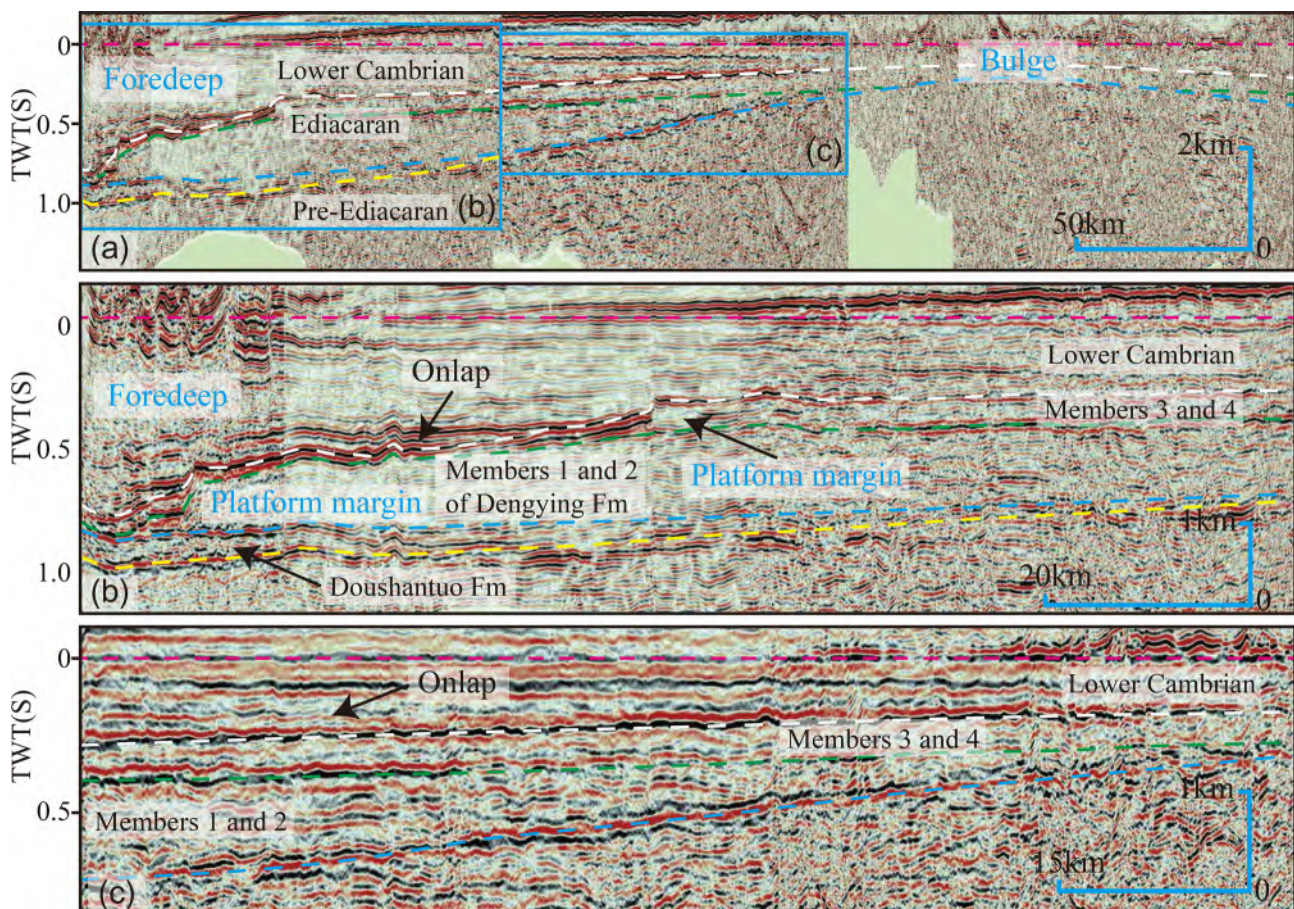


**Fig. 4.** Regional seismic reflection profile (*c.* 400 km long) across the Sichuan Basin from NW to SE. The seismic profile is presented by levelling the top of the Lower Cambrian (dashed pink line), and the location is shown in Figure 1. The dashed white line denotes the boundary between the Ediacaran and the Cambrian, which is also an unconformity surface on the platform part of the Ediacaran Dengying Formation. (a) General seismic reflection profile, showing the structure of the platform margins in the Ediacaran and the foreland in the Lower Cambrian. Vertical exaggeration is about 15 times. (b) Exaggerated seismic reflection profile in the NW Sichuan Basin, showing two platform margins in the Ediacaran and a foredeep in the Lower Cambrian. Vertical exaggeration is about eight times. (c) Exaggerated seismic reflection profile in the central Sichuan Basin, showing onlap of the Lower Cambrian from NW to SE. Vertical exaggeration is about eight times.

grains therein are dominated by plagioclase with rare K-feldspar. Lithic fragments are mainly composed of chert and carbonate rock detritus (Fig. 9). Some samples also contain a certain amount of metamorphic lithic fragments, such as quartzite and schist. The framework grain composition (Q–F–L) ternary plot demonstrates that the Kangjiagou section sandstones were mainly derived from a recycled orogenic source (Fig. 10a). It should be noted that the samples with high lithic fragment content (>70%), which plot in the arc source fields, are very coarse-grained sandstones and these sandstones are also rich in sedimentary lithic fragments (e.g. chert).

**Heavy minerals**

The transparent heavy mineral assemblages of the Canglangpu Formation sandstone samples from the Kangjiagou section are dominated by zircon, tourmaline, chlorite and epidote. Biotite, rutile, garnet and barite are also common in these analysed sandstones and display comparatively high abundances in some samples (Fig. 10b). The heavy minerals in the samples show highly variable textures. These grains are poorly sorted (ranging from 30 to 250 μm in sizes) and are angular to rounded in shape.

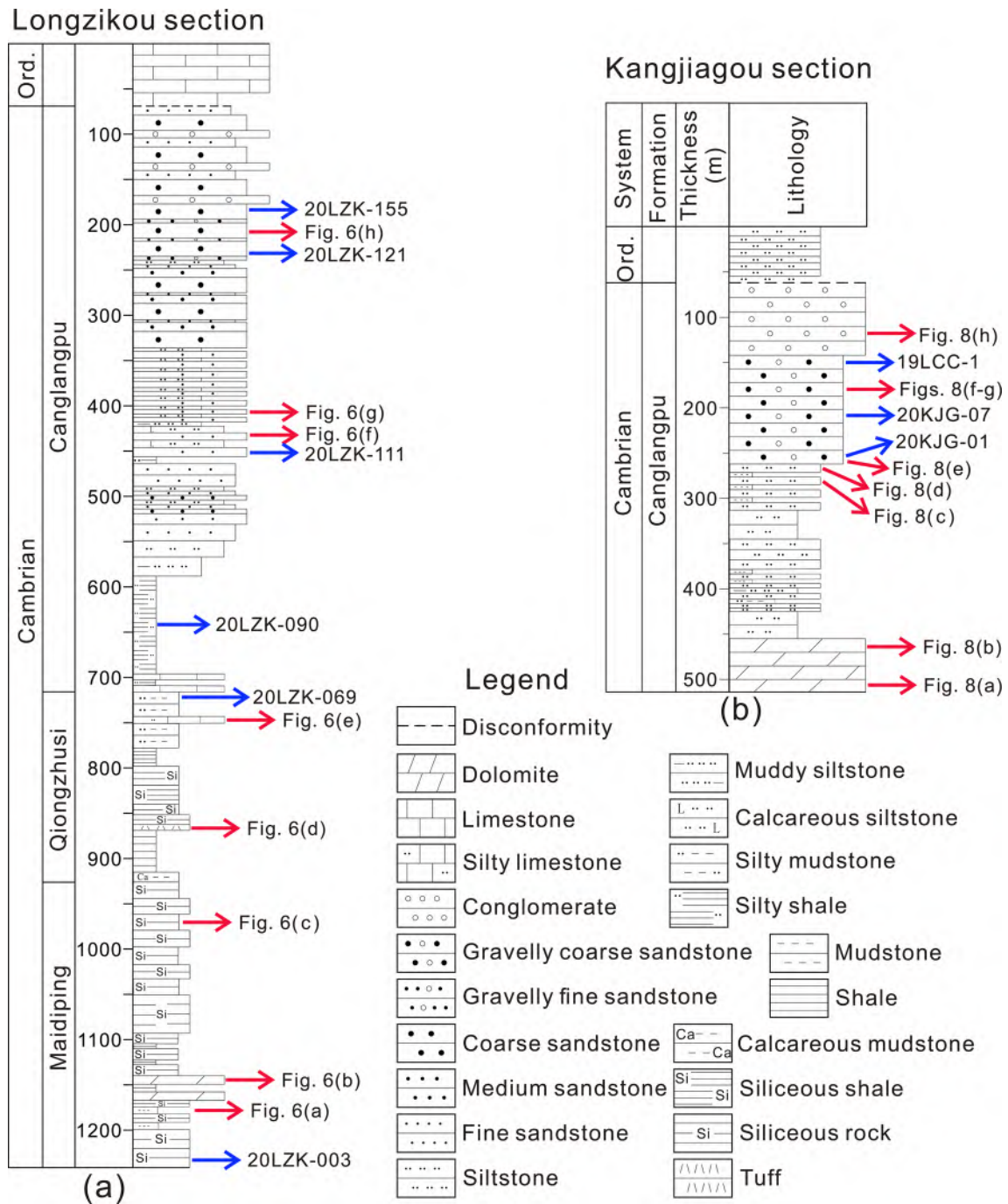


**Fig. 5.** Generalized lithostratigraphic columns for the Lower Cambrian outcrops of the Longzikou and Kangjiagou sections. (a) The Longzikou section contains the Maidiping, Qiongzhusi and Canglangpu formations, which show an overall coarsening-upward succession from shale to conglomerate and indicate a tectonic transition from a passive margin to an active foreland setting; the Canglangpu Formation is unconformably overlain by the Ordovician. (b) The Kangjiagou section only exposes the Canglangpu Formation showing an overall coarsening-upward succession; the top of the Canglangpu Formation is dominated by thick coarse-grained sandstone with conglomerate and massive conglomerate, which indicates an intense uplift tectonic event in the nearby source region. Red arrows point to the locations of the photographs in Figures 6 and 8, and blue arrows point to the locations of collected samples.



**Fig. 6.** Representative outcrop photographs of the Lower Cambrian at the Longzikou section, Beichuan County. (a) Black thin-bedded siliceous shale from the lower Maidiping Formation. (b) Interbedded thin dolomite and chert from the lower Maidiping Formation. (c) Black thin-bedded siliceous shale with pyrite nodules in the upper part of the Maidiping Formation. (d) A volcanic ash bed interlayered with black shale in the Qiongzhusi Formation. (e) A medium limestone bed interlayered with thin-bedded mudstone, in the upper part of the Canglangpu Formation. (f) Thin to medium siltstone, in the middle Canglangpu Formation, showing a small-scale coarsening-upward sequence. (g) Current ripples from the sandstone in the middle Canglangpu Formation showing a SE-vergent palaeocurrent direction (oriented at 120°). (h) Thick coarse-grained sandstone with minor conglomerate in the upper Canglangpu Formation.

Compositionally, the heavy minerals are moderately to highly mature and have variable, medium to high ZTR values (ranging from 33 to 94,  $ZTR\ Index = 100 \times (\text{zircon} + \text{tourmaline} + \text{rutile}) / \text{all transparent heavy minerals}$ ).

### Major, trace and rare earth element composition

The raw data for major, trace and rare earth elements in the analysed samples from the Longzikou section are shown in the [Supplementary material](#). The major elements mainly include Si ( $\text{SiO}_2$  37–77 wt%), Al ( $\text{Al}_2\text{O}_3$  6–21 wt%), Fe ( $\text{Fe}_2\text{O}_3$  0.3–8.4 wt%), Na ( $\text{Na}_2\text{O}$  0.7–5.3 wt%) and K ( $\text{K}_2\text{O}$  1.0–5.0 wt%). Calcium is depleted in Maidiping Formation and Qiongzhusi Formation samples and displays relatively high contents in Canglangpu Formation samples. Upper continental crust (UCC) composition-normalized element patterns of all the analysed Lower Cambrian samples are shown in [Figure 11](#). Overall, most analysed samples display remarkable depletion in Ca (CaO contents average 1.9 wt% and are less than 0.1 wt% for some Maidiping Formation and Qiongzhusi Formation samples) and Sr and moderate depletion in Zr and Hf, relative to UCC. All the samples indicate light rare earth element enrichment and relatively flat heavy rare earth element patterns and have slightly to moderately negative Ce and Eu anomalies, relative to the chondrite

compositions. The trace element-based tectonic setting discrimination ternary plots (i.e. La–Th–Sc and Th–Sc–Zr/10 ternary diagrams, from [Bhatia and Crook 1986](#)) indicate that most of the analysed samples from the Longzikou section can be plotted in or near the continental island arc field ([Fig. 12](#)). Binary plots and stratigraphic variations of representative element concentrations and element ratios of the samples are illustrated in [Figures 13 and 14](#), respectively. Most Maidiping Formation and Qiongzhusi Formation samples are obviously rich in Ba (most contain 2000–50 000 ppm), U (mostly 4–16 ppm), V (mostly 200–1700 ppm) and Mo (mostly 8–100 ppm), compared with the Canglangpu Formation samples ([Fig. 14](#)). The Maidiping Formation and Qiongzhusi Formation samples have slightly higher Zr (averaging 133 ppm) and Hf (averaging 4.0 ppm) contents, higher Zr/Sc, V/Cr, V/(V + Ni) and U/Th ratios and lower Ce/Ce\* values than the Canglangpu Formation samples ([Fig. 14](#); Zr and Hf average 66 and 2.3 ppm, respectively).

### U–Pb ages and Lu–Hf isotopes

#### U–Pb dating of detrital zircons

All of the zircon grains from Longzikou section samples (20LZK-111, 20LZK-121 and 20LZK-155) have oscillatory zoning, with the

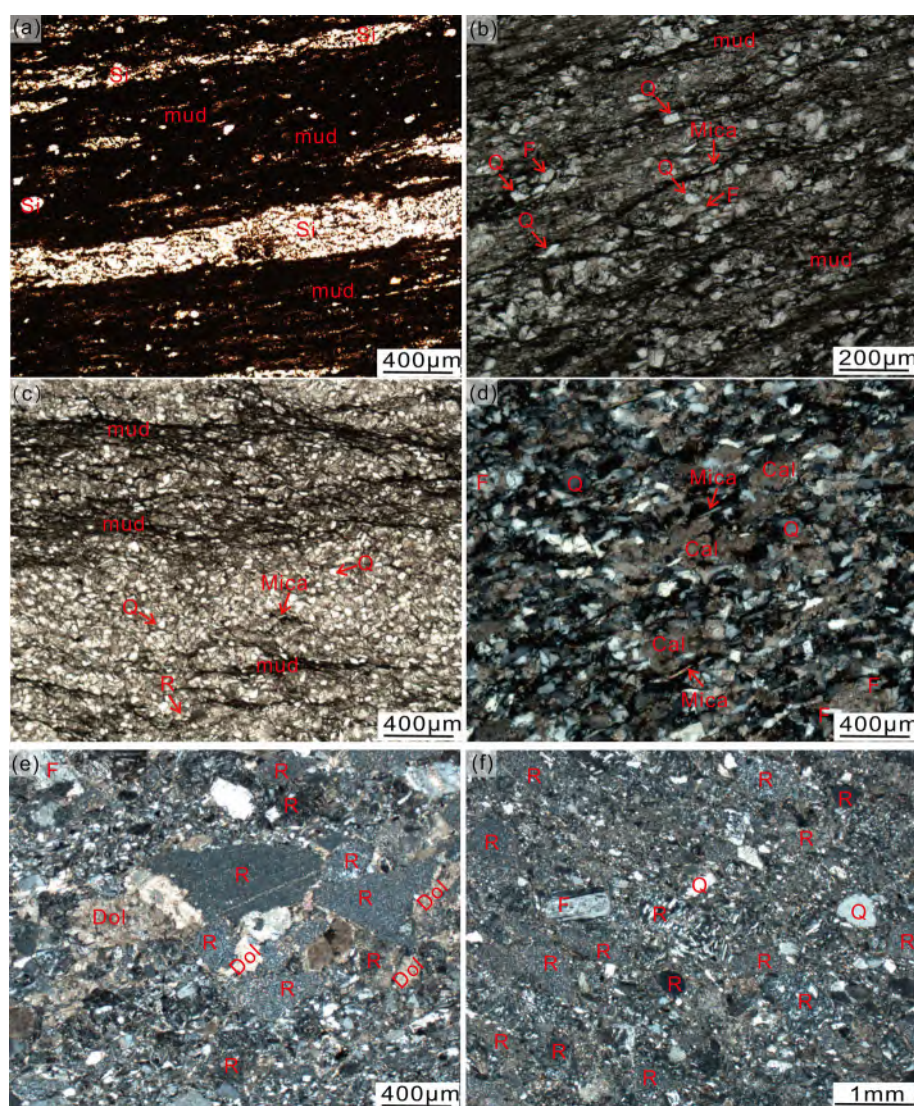


**Fig. 7.** Photomicrographs of sedimentary rocks from the Longzikou section. (a) Interbedded chert and mudstone. Sample 20LZK-003 from bottom of the Maidiping Formation; plane-polarized light (PPL). (b) Silty mudstone, mainly composed of mud bands and silt-sized silica debris. Sample 20LZK-069 from top of the Qiongzhusi Formation; PPL. (c) Interbedded laminae of mud, silt sands and calcite silt sands, showing features of tidal rhythms. Sample 20LZK-90 from the lower part of the Canglangpu Formation; PPL. (d) Calcitic siltstone, containing abundant feldspar, rock fragments and quartz. Many grains have been replaced by calcite. Some calcite patches contain residual quartz grains. Sample 20LZK-111 from the middle part of the Canglangpu Formation; cross-polarized light (XPL). (e) Calcite- and pebble-bearing coarse sandstone, poorly sorted and poorly rounded, containing various sedimentary, metamorphic and volcanic rock fragments, silt- to coarse-sized quartz and calcification grains. Sample 20LZK-121 from the upper part of the Canglangpu Formation; XPL. (f) Calcite-bearing medium to coarse sandstone, mainly composed of various rock fragments, feldspar and quartz. Sample 20LZK-155 from the upper part of the Canglangpu Formation; XPL. Si, opal and chert; Q, quartz grains and crystals; Dol, dolomite crystals and dolomite grains; Cal, calcite; R, rock fragments; F, feldspar; mica, mica. The positions of the samples in the section are shown in Figure 5.

majority of Th/U values between 0.12 and 1.96, typical of magmatic zircon. A total of 100 zircon grains were analysed for each sample and more than 95% of zircons therein have concordant ages (discordance between  $^{206}\text{Pb}/^{238}\text{U}$  and  $^{207}\text{Pb}/^{235}\text{U}$  ages <10%). The three analysed samples have similar detrital zircon age populations. The age spectra are dominated by a strong peak in the Early Cambrian at *c.* 530 Ma, covering more than 40% of grains for each sample (Fig. 15). The majority of other grains are mainly Neoproterozoic, with ages between 566 and 1075 Ma. A smaller proportion of zircon grains belong to the Neoproterozoic to early Paleoproterozoic from 2.4 to 2.6 Ga, with weak age peaks at *c.* 2.5 Ga.

Zircon grains from the three Kangjiagou samples (20KJG-01, 20KJG-07 and 19LCC-01) show magmatic features with oscillatory zoning and the majority of Th/U values between 0.17 and 1.86. In total, 100 zircon grains were analysed for each sample, and only a few grains are less than 10% discordant. Of 96 zircon grains after ruling out the discordant grains, 67 grains in sample 20KJG-01 spread between 618 and 1093 Ma, with a strong peak at 853 Ma and a secondary peak at 768 Ma as well as two minor peaks at 977 and 644 Ma (Fig. 16a and b). The other grains have Late Neoproterozoic to Paleoproterozoic ages, from 2.69 to 1.9 Ga, with a weak peak at 2.46 Ga. The majority of zircon grains in sample 20KJG-07 spread between 510 and 1041 Ma, with a prominent peak at *c.* 826 Ma and some minor peaks at *c.* 545, 529 and 984 Ma (Fig. 16c and d). Four of the other grains showed ages between 1.76 and 2.01 Ga, and the

other 11 grains have Neoproterozoic to Paleoproterozoic ages with a weak peak at 2.49 Ga, two of which yield a Paleoproterozoic age of *c.* 3.2 Ga. The age spectrum of sample 19LCC-01 spread between 536 Ma and 3.29 Ga. The majority of zircon grains spread between 536 and 1053 Ma, with a prominent peak at *c.* 825 Ma and some minor peaks at *c.* 624, 855 and 755 Ma (Fig. 16e and f). Only one grain yields a Mesoproterozoic age (i.e. 1231 Ma). Twenty-five zircon grains have Paleoproterozoic ages without obvious peaks. Fifteen zircon grains yield an Archean age from 2.52 to 3.29 Ga, with two peaks at 2.52 and 2.68 Ga.

#### Lu–Hf isotopes

Lu–Hf isotopic data were collected from five samples that were analysed for U–Pb isotopes with concordant ages to determine the provenance of the protoliths for the sedimentary rocks in the Longmenshan fold–thrust belt. The Hf isotopic results are presented in an  $\epsilon_{\text{Hf}}$  v. age diagram in Figure 17 and the raw data are shown in the Supplementary material. The results demonstrate that the detrital zircons with Cambrian and Neoproterozoic ages have wide ranges of  $\epsilon_{\text{Hf}}$  values ( $\epsilon_{\text{Hf}}$  values of the 518–545 Ma zircons from sample 20LZK-111, the 493–560 Ma zircons from sample 20LZK-155 and the 510–545 Ma zircons from sample 20KJG-07 are between –22.05 and –2.09, between –31.47 and 5.11 and between 3.76 and 9.75, respectively). The early–middle Neoproterozoic detrital

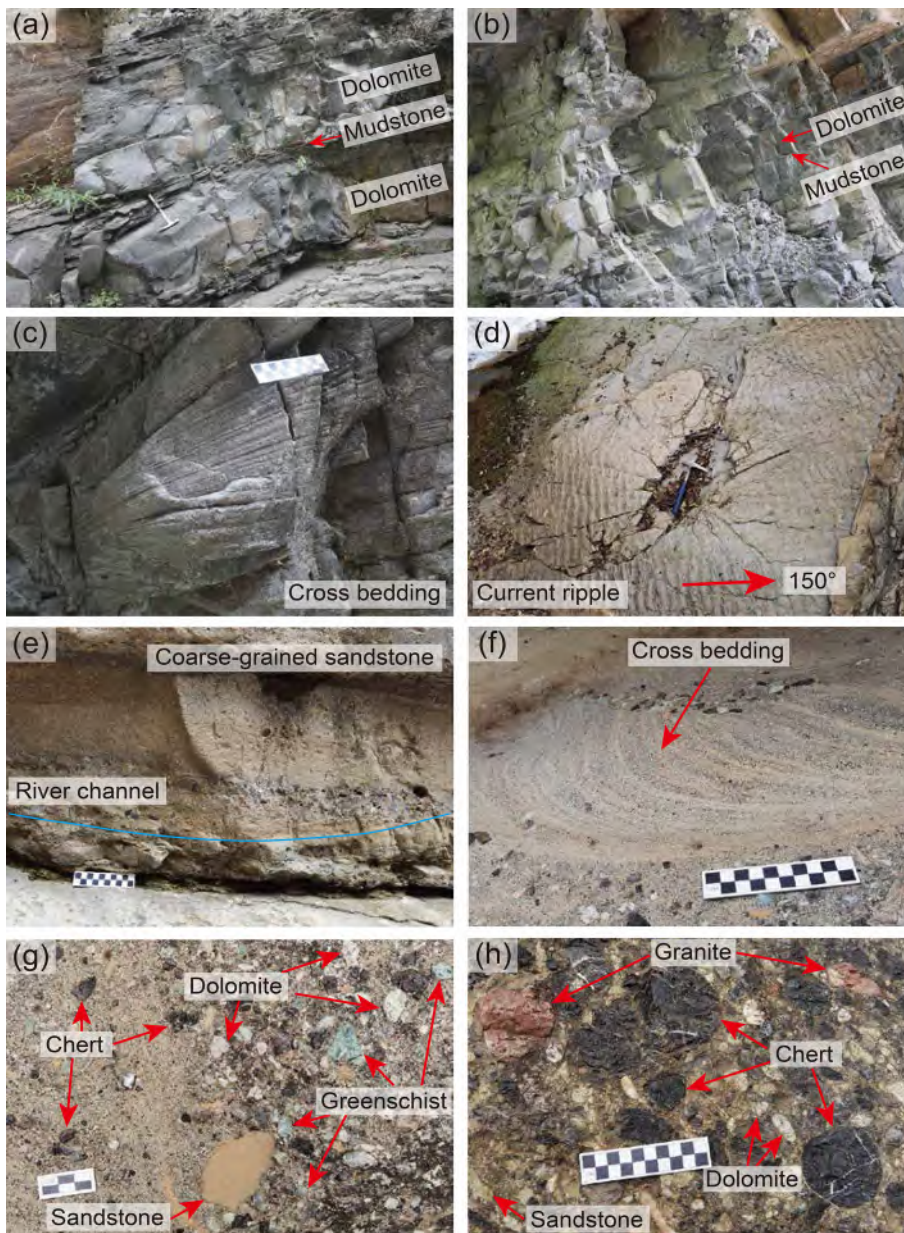


**Fig. 8.** Representative field outcrop photographs of the Lower Cambrian Canglangpu Formation at the Kangjiagou section. (a, b) Medium to thick dolomite interbedded with thin mudstone at the base of the Canglangpu Formation. (c) Cross-bedding from the sandstone showing a SE-vergent palaeocurrent direction. (d) Current ripples from siltstone 2 m below the coarse-grained sandstone showing a SE palaeocurrent direction. (e) Base of the coarse-grained sandstone developed in a river channel environment. (f) Cross-bedding from coarse-grained sandstone with conglomerate showing a SE-vergent palaeocurrent direction. (g) Conglomerate layers within the coarse-grained sandstone are mainly composed of black chert, green greenschist, light carbonate and brown sandstone, indicating immaturity and a proximal sediment source. (h) The components within the massive conglomerate are mainly black chert, red granite and smaller dolomite and sandstone. The positions of the photographs are shown in Figure 5b.

zircon  $\epsilon_{\text{Hf}}$  values range from  $-23.28$  to  $14.86$ . Furthermore, most of the analysed Early Paleoproterozoic zircon ages have negative  $\epsilon_{\text{Hf}}$  values and the Archean zircon grains have both positive and negative  $\epsilon_{\text{Hf}}$  values (Fig. 17).

## Discussion

### *Provenance of the Lower Cambrian siliciclastic rocks in the NW Yangtze Block*

After deposition of the Ediacaran Dengying Formation, the NW Yangtze Block was almost fully covered by marine carbonate rocks forming a unified carbonate platform across the block. The thick clastic succession of the Lower Cambrian, however, was well developed in the NW Yangtze Block, spreading to the east. Determination of the provenance of the Lower Cambrian clastic rocks is of importance for understanding the tectonic affinity and evolution of the NW Yangtze Block. Some researchers considered that the Paleozoic sedimentary rocks in South China were derived from the SE blocks (Wang *et al.* 2010; Shu *et al.* 2014). For example, Shu *et al.* (2014) suggested that the Cambrian to Ordovician sequences in NW Cathaysia were sourced from the

east to SE. It is generally accepted that the Yangtze Block was separated from the Cathaysia Block by an intracontinental abyssal basin during the Ediacaran to Cambrian (Wang *et al.* 2010; Jiang *et al.* 2011; Li *et al.* 2018). In this case, terrestrial clastic sediments would be impeded by the abyssal basin and could not be transported into the western Yangtze Block, implying a low possibility of sedimentary sources from the east or SE. Another viewpoint favours an origin of the clastic sediments from some distal exotic terranes, such as north India and the Himalaya (Yao *et al.* 2014; Chen *et al.* 2016, 2018). For example, Chen *et al.* (2016) investigated the provenance of the Silurian–Devonian rocks in the west Yangtze Block using U–Pb age and Hf isotopic data of detrital zircons, and suggested an exotic source of the sediments derived from the northwestern margin of the supercontinent Gondwana. Their evidence includes the occurrence of some dominant zircon ages ( $0.9$ – $1.0$ ,  $0.73$ – $0.85$ ,  $0.49$ – $0.67$  and  $2.5$  Ga), which were considered to be not widely present in South China, and the moderately to highly rounded shapes of the zircon grains (Chen *et al.* 2016, 2018).

In this study, we integrated seismic and well data from gas exploration activities in the Sichuan Basin with some representative outcrops in the NW Yangtze Block, using sedimentological,

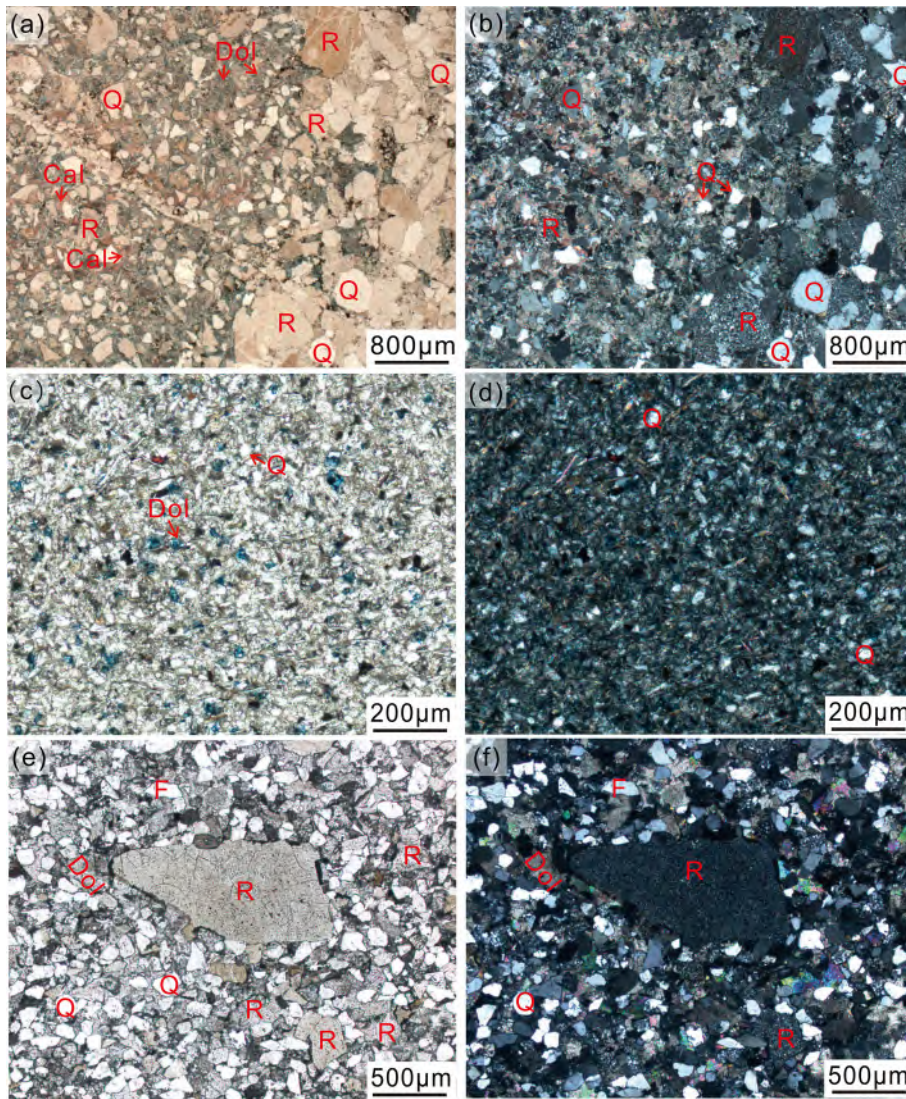


**Fig. 9.** Photomicrographs of detrital zircon dating samples from the Kangjiagou section. (a) Calcitic conglomeratic litharenite. The grains are mainly metamorphic and volcanic rock fragments and quartz, cemented by calcite (stained red) and ferrodolomite (stained blue). Sample 20KJG-01; PPL. (b) The same field of view as in (a). The rock fragments are mainly siliceous rocks, carbonate rocks and volcanic rocks; XPL. (c) Siltstone, mainly composed of very fine quartz, mica grains and carbonate cements. The ferrodolomite is stained blue. Sample 20KJG-07; PPL. (d) The same field of view as in (c). Many grains showing complete extinction are amorphous silicon; XPL. (e) Dolomitic conglomeratic litharenite. The grains are mainly sand-size rock fragments and quartz, with minor angular pebbles and coarse rock fragments. Mica and some silty to fine-grained heavy minerals including zircons are also observed. Sample 19-LCC; PPL. (f) The same field of view as in (e). The conglomerates are poorly sorted, with low compositional maturity; XPL. Q, quartz grains and crystals; Dol, dolomite cements; R, rock fragments.

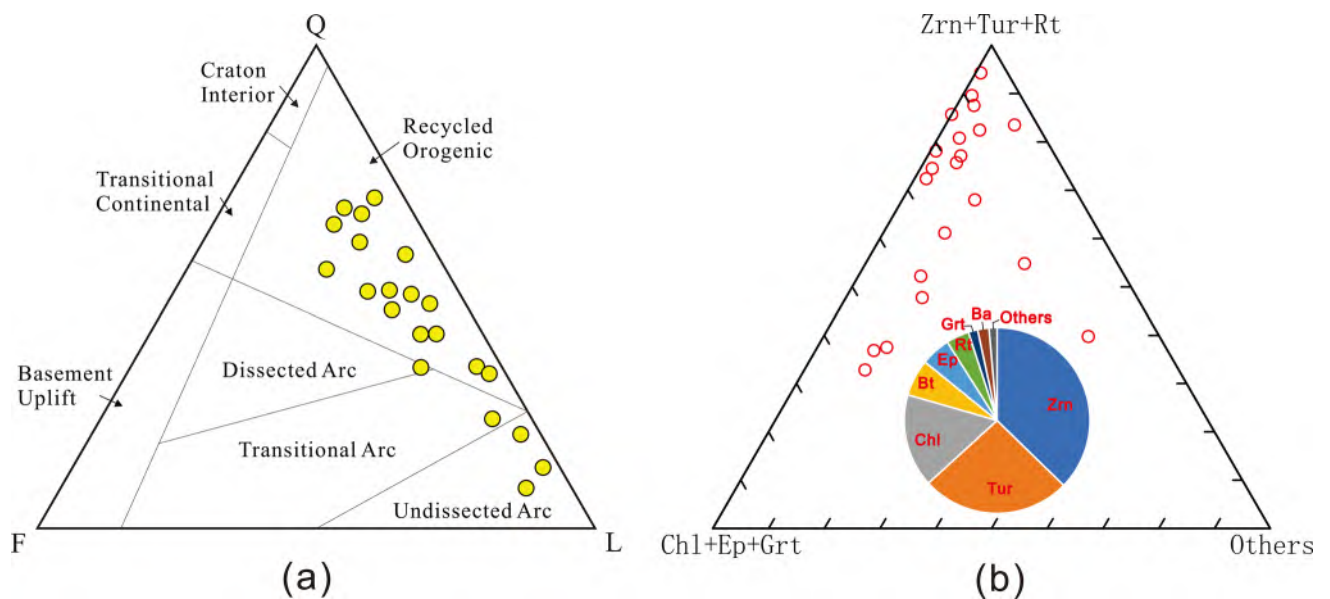


**Fig. 10.** Sandstone framework grain and heavy mineral compositions of the Canglangpu Formation from the Kangjiagou section. (a) Q-F-L (quartz-feldspar-lithic fragment) ternary diagram for tectonic setting discrimination (interpretation fields from Dickinson 1985). (b) A ternary diagram (Zrn + Tur + Rt - Grt + Ep + Chl - Others) showing the variability of heavy mineral assemblages. The pie chart indicates the average heavy mineral compositions of all the samples from this section. Zrn, zircon; Tur, tourmaline; Rt, rutile; Chl, chlorite; Ep, epidote; Grt, garnet. Other minerals, as the minor components of the heavy mineral assemblages, mainly include hornblende, augite, apatite, monazite, biotite and barite. It should be noted that most samples plot in the recycled orogenic field and the samples with extremely high lithic fragment contents are very coarse-grained sandstones. Heavy minerals in the Canglangpu Formation sandstones are dominated by zircon, tourmaline, chlorite, biotite, epidote and rutile.

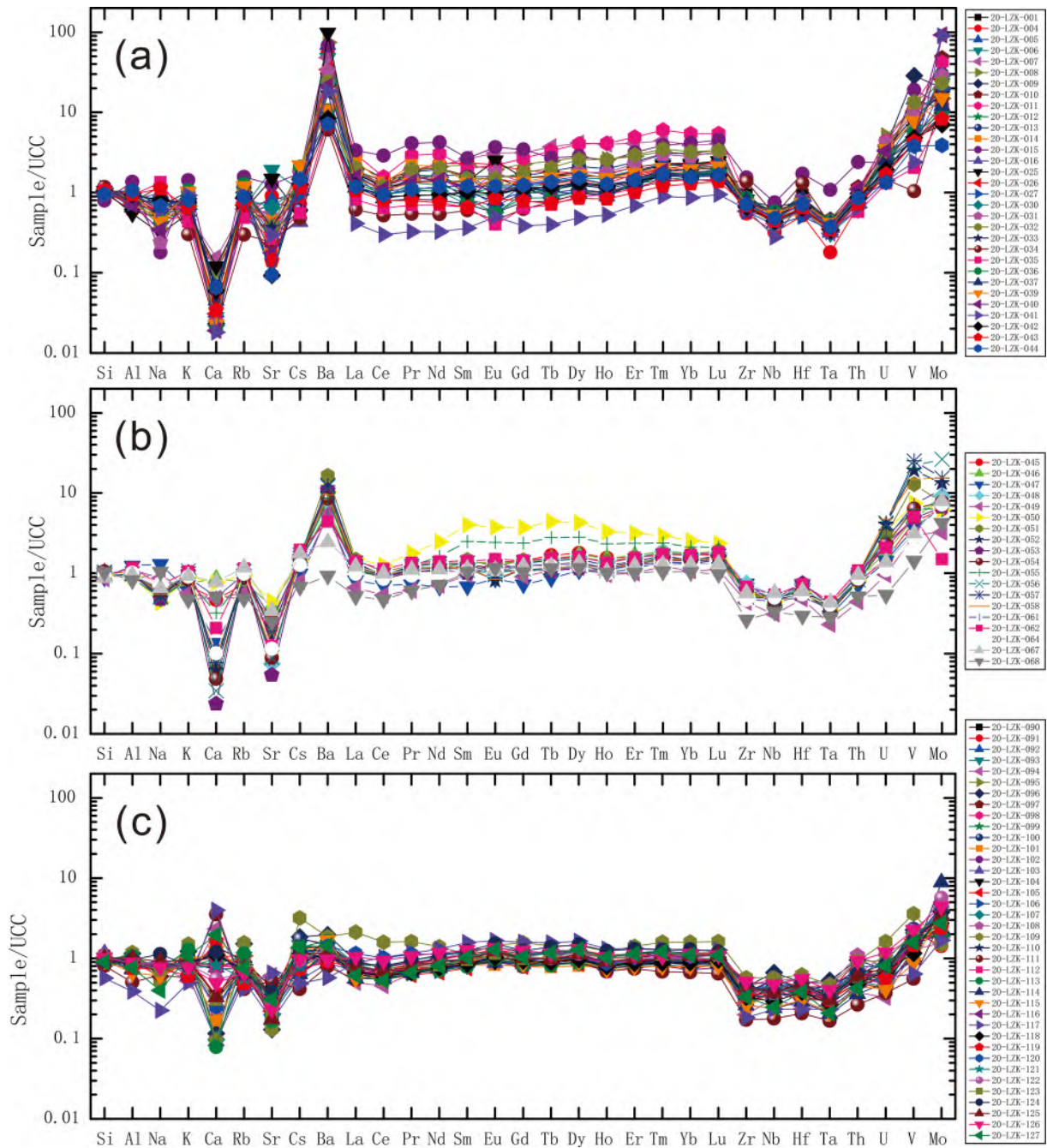


**Fig. 11.** Upper continental crust (UCC) normalized element patterns of Maidiping Formation (a), Qiongzhusi Formation (b) and Canglangpu Formation (c) samples from the Longzikou section. UCC composition data are from Taylor and McLennan (1985).

petrological, geochemical and detrital zircon U–Pb–Hf isotopic analyses, to decipher the provenance of the Lower Cambrian clastic rocks in the NW Yangtze Block. Palaeocurrent measurements based on current ripples, cross-bedding and conglomerate gravel imbrications are an effective way to determine the direction of sediment transport pathways. The measurement results show an overall present-day SE-vergent palaeocurrent direction, indicating that the NW regions were most probably closer to the detrital sources than were the SE regions. The regional seismic profile across the Sichuan Basin shows northwestward thickening and southeastward thinning of the Lower Cambrian within the basin, indicating that sediments were derived from the NW, consistent with the palaeocurrent measurements. The lithostratigraphic correlation of the Lower Cambrian across the Yangtze Block reveals that the Bikou terrane may provide the source of the Lower Cambrian clastic rocks deposited in the Longmenshan and Sichuan Basin. The petrological

observations of the Lower Cambrian Canglangpu Formation sandstones demonstrate that the clastic rocks are dominated by immature components, especially the development of volcanic components and conglomerates, indicating a proximal source, rather than a distal source. The massive conglomerate succession at the top of the Canglangpu Formation at the Kangjiaguo section shows dominant immature and proximal features, and the clasts within the conglomerate are dominated by chert, carbonate rocks and metasedimentary rocks, which is consistent with the framework grain compositions of the analysed sandstones. All the provenance evidence reveals that the neighbouring Bikou terrane could be an important contributor to the sedimentary succession.

Heavy mineral analysis results indicate highly variable textures and medium to high ZTR values of the heavy mineral grains, revealing that these clasts could be contributed by both proximal igneous rocks and recycling of underlying sedimentary successions

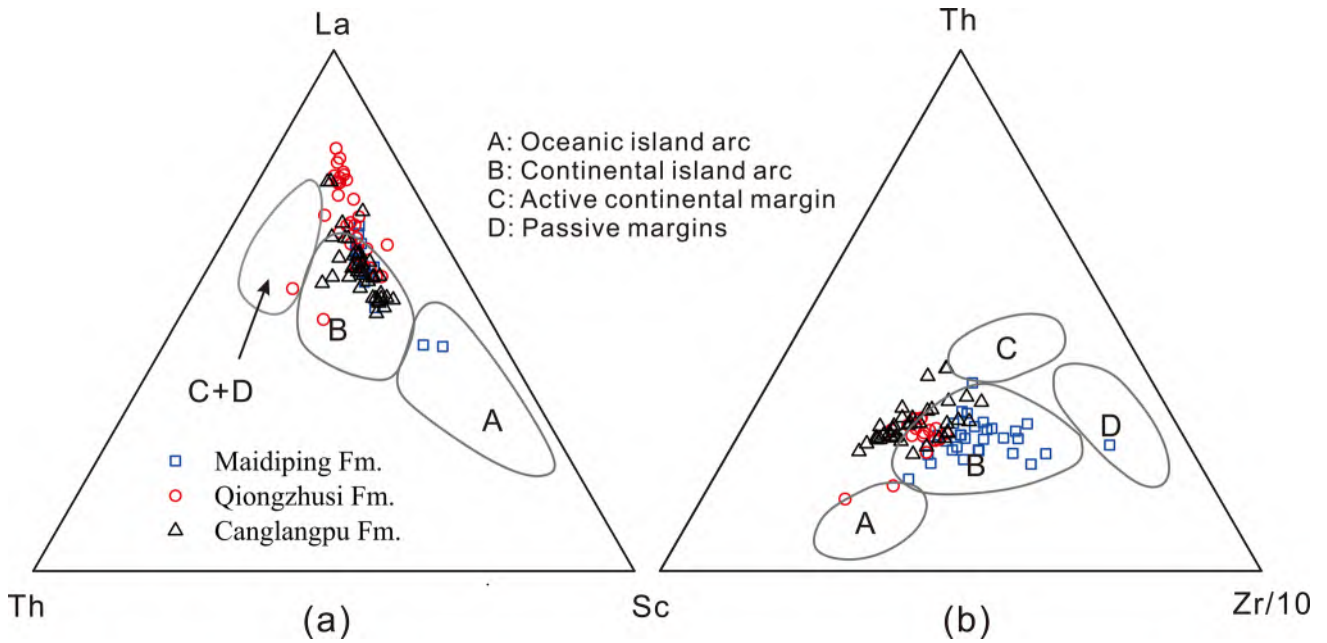


**Fig. 12.** Trace element-based tectonic setting interpretations for the analysed fine-grained sedimentary rock samples from the Longzikou section. (a) La–Th–Sc ternary diagram and (b) Th–Sc–Zr/10 ternary diagram (after Bhatia and Crook 1986).

in adjacent regions. The trace and rare earth elements, such as La, Th, Sc, Zr and Hf and related element ratios, suggest variable parent-rock types for the Maidiping and Qiongzhusi Formation sediments (e.g. felsic and mixed felsic–mafic rocks) and dominant felsic parent-rocks for the Canglangpu Formation sediments (Fig. 13b). Furthermore, the Maidiping and Qiongzhusi Formation sediments indicate comparatively more intense signals of sedimentary recycling than the Canglangpu Formation sediments (Fig. 13a).

Detrital zircon U–Pb dating could provide important information on sedimentary provenances, and Lu–Hf isotopic analysis may offer insights into the nature and source of magmatic rocks in the provenance of the sediments (Chen *et al.* 2018). The age spectra of detrital zircons from the Canglangpu Formation at the Longzikou

section show a prominent peak at *c.* 530 Ma, close to its deposition age of *c.* 510 Ma, which is further indicative of a proximal source. The *c.* 750–830 Ma zircons have been demonstrated to have a proximal magmatic source, and are well developed in the NW Yangtze Block (Chen *et al.* 2016, 2018). The *c.* 970 Ma age of detrital zircons from the Canglangpu Formation in the Longzikou section has been reported in the Tongmuliang Group in the northwestward Jiaoziding complex by Li *et al.* (2018), consistent with a NW-derived proximal source. The *c.* 2.5 Ga detrital zircons may be derived from an old basement nearby, indicating that an older continental crust existed to the NW. The positive  $\epsilon_{\text{Hf}}(t)$  values with the age *c.* 530 Ma indicate that the magmatic source was derived from a depleted mantle. The age spectra of detrital zircons

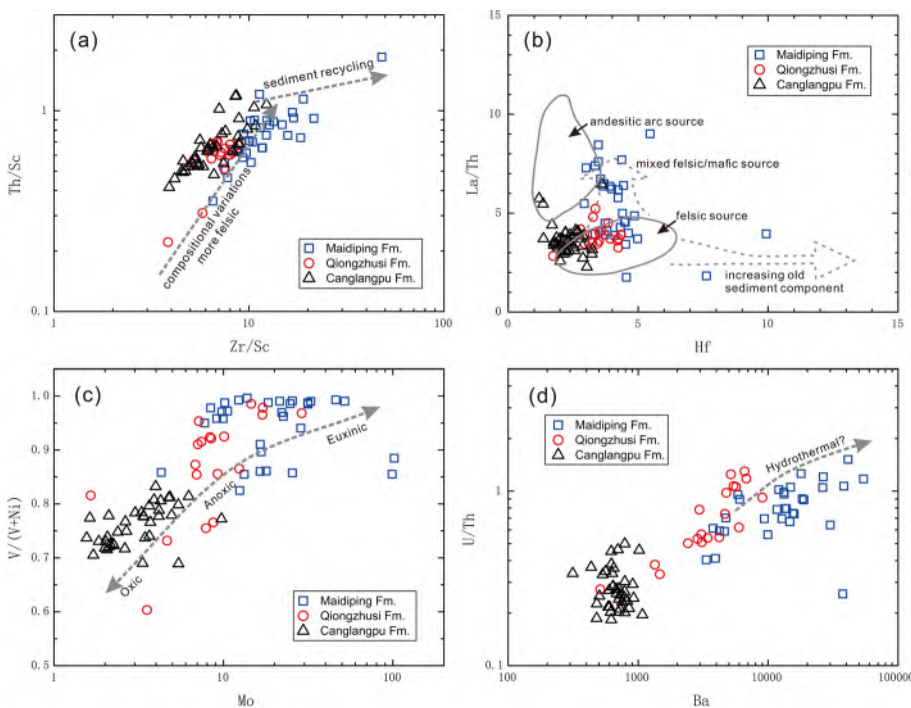


**Fig. 13.** Binary diagrams of representative element concentrations and element ratios of the analysed samples from the Longzikou section. (a) Th/Sc v. Zr/Sc (after McLennan *et al.* 1993); (b) La/Th v. Hf (after Floyd and Leveridge 1987); (c) V/(V + Ni) v. Mo; (d) U/Th v. Ba.

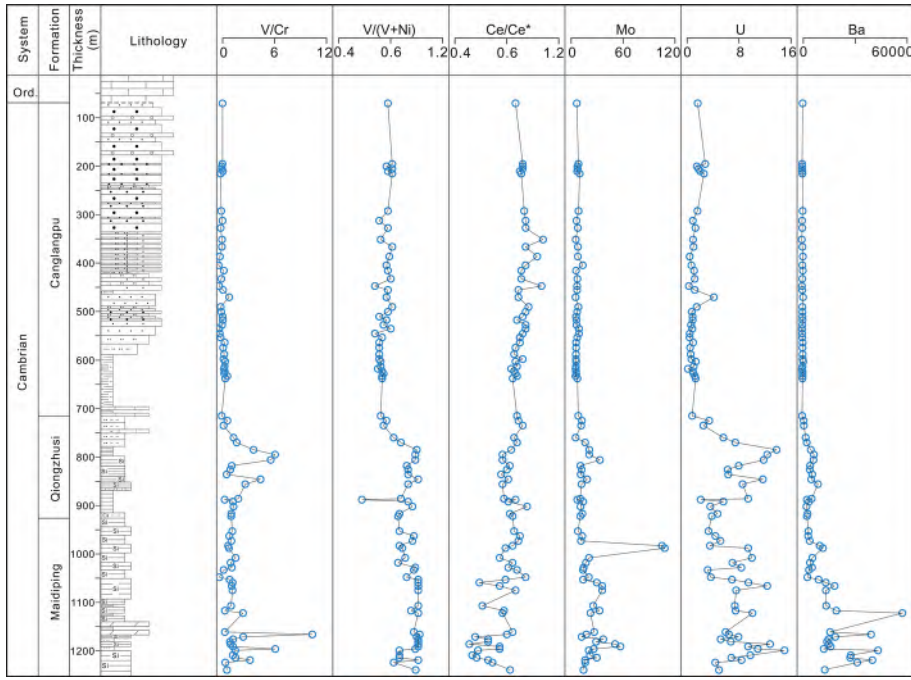


**Fig. 14.** Vertical variations of representative element concentrations and element ratios of the analysed Longzikou section samples. Ce-anomaly is represented as  $Ce/Ce^* = Ce_N / (La_N \times Pr_N)^{1/2}$ , based on chondrite-normalized values. CI carbonaceous chondrite compositions (Taylor and McLennan 1985) were used for the normalization.

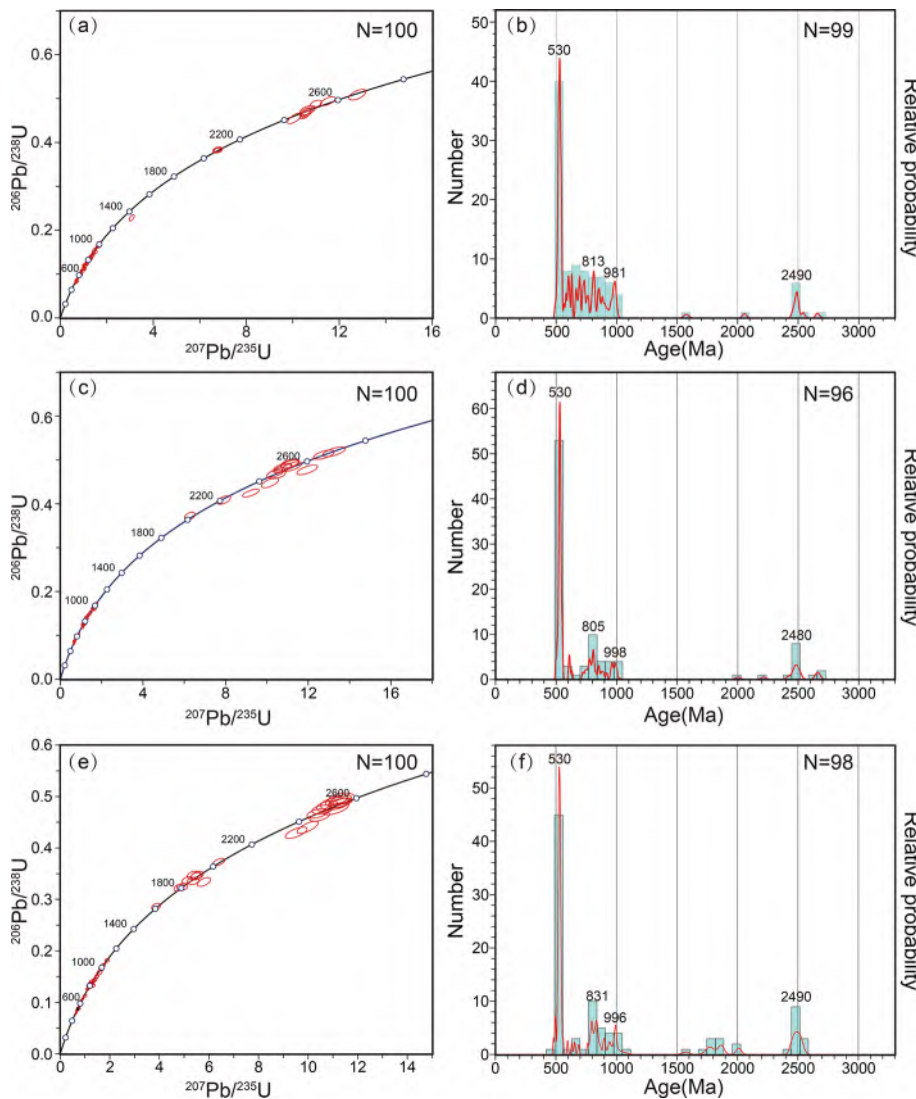


**Fig. 15.** Concordia plots (a, c, e) and histogram as well as relative probability plots (b, d, f) of LA-ICP-MS detrital zircon U-Pb age distributions from the Canglangpu Formation sandstone samples at the Longzikou section. The  $^{207}Pb/^{206}Pb$  age is used for zircons older than 1000 Ma and  $^{206}Pb/^{238}U$  age is used for zircons younger than 1000 Ma. Analyses are plotted with  $2\sigma$  error ellipse after common-Pb correction. Sample locations are shown in Figure 5a. (a, b) Sample 20LZK-111; (c, d) sample 20LZK-121; (e, f) sample 20LZK-155.

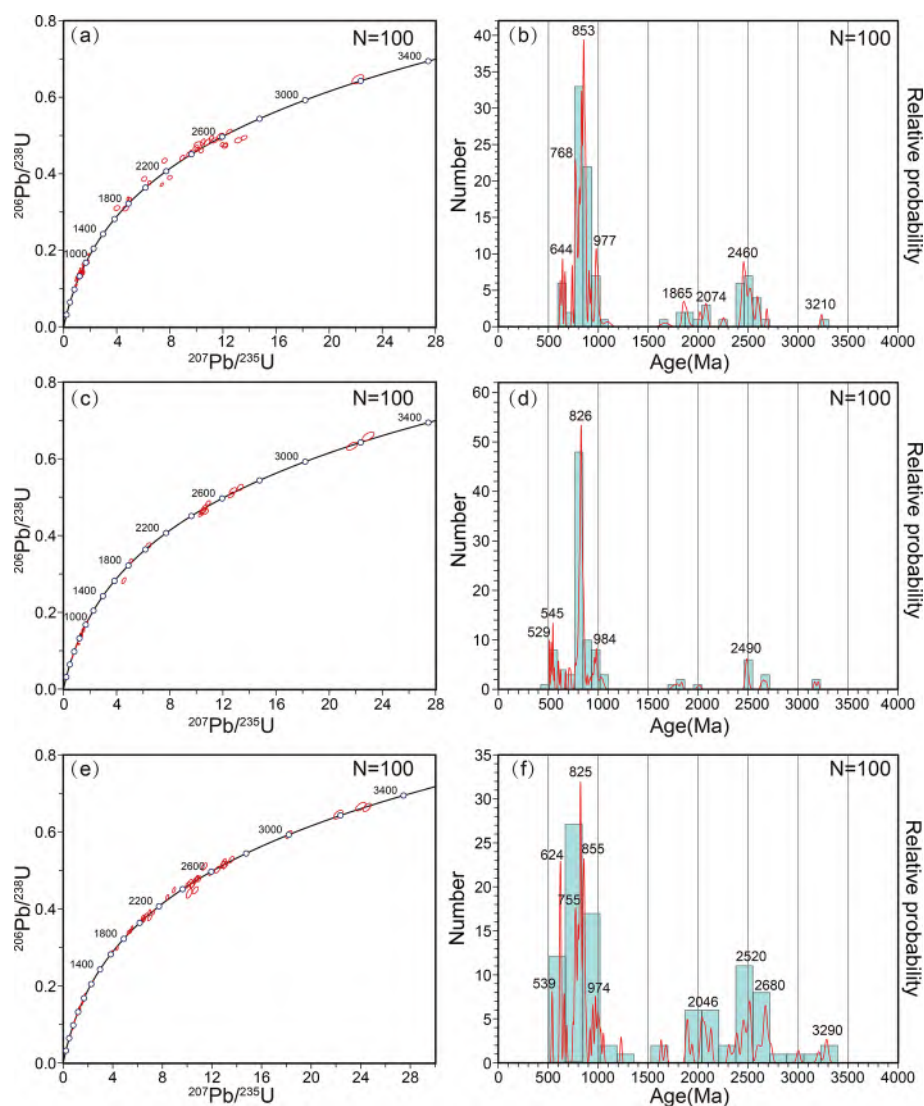


**Fig. 16.** Detrital zircon U–Pb age plots for the Canglangpu Formation sandstones of the Kangjiagou section. Sample locations are shown in Figure 5b. (a, c, e) U–Pb concordia diagrams of detrital zircon; (b, d, f) relative probability diagrams of zircon U–Pb ages. (a, b) Sample 20KJG-0; (c, d) sample 20KJG-07; (e, f) sample 19LCC-01.

from the Canglangpu Formation in the Kangjiagou section show a different pattern from those in the Longzikou section. The dominant age peak is *c.* 826 Ma, consistent with the development of Neoproterozoic magmatism in the western Yangtze Block. A minor *c.* 530 Ma age peak indicates an Early Cambrian tectono-magmatic event in the nearby source region. The occurrence of *c.* 980 Ma zircons indicates a source from the Jiaoziding complex and northwestward regions. The occurrence of *c.* 2.5 Ga zircons shows a common feature with those of the Longzikou section. Moreover, the occurrence of *c.* 3.2 Ga zircons with positive  $\varepsilon_{\text{Hf}}(t)$  values shows a juvenile Paleoproterozoic continental crust, consistent with the Paleoproterozoic Yudongzi Group, which occurs in the NW Yangtze Block (Zhang *et al.* 2001).

In summary, the Lower Cambrian clastic rocks in the NW Yangtze Block appear to be from local sources to the NW, such as the Jiaoziding complex, the Bikou terrane, the West Qinling orogen and even the buried present-day Songpan–Ganzi terrane.

#### ***Tectonic transition from a passive margin to a foreland basin***

The Ediacaran succession comprising the Doushantuo and Dengying formations in South China is dominated by thick marine carbonate rocks interlayered with minor clastic rocks, which are generally considered to have formed in a passive margin setting (Zhou and Xiao 2007; Jiang *et al.* 2011; Zhou *et al.* 2019; Gu

*et al.* 2021). The Lower Paleozoic sequence in the NW Yangtze Block has long been considered to be also formed in a passive margin setting (Meng and Zhang 1999; Dong and Santosh 2016; Domeier 2018). Chen and Yang (2000), however, argued that a long-term active continental margin with intense tectonic activity existed in the Paleozoic, based on the chemical composition of sedimentary rocks.

From the Ediacaran to the Cambrian, considerable variations occurred as a result of tectonic and sedimentary environment changes. One of the important variations is the decrease of marine carbonate rocks and the significant increase of clastic rocks in the Lower Cambrian, which from base to top shows an obvious reverse grading, from fine-grained to coarse-grained texture and from thin to medium-thick bedding, indicating a tectonic transition from a former passive margin setting to an active margin setting. The sediments of the Lower Cambrian show dominantly immature features, together with the occurrence of thick conglomerates and proximal, local sources, revealing that a possible uplift event occurred to the NW. The Lower Cambrian succession in the Sichuan Basin thickens dramatically to the NW, indicating basin subsidence as a result of loading to the NW of the present-day Longmenshan, where collisional orogens may occur, resulting in the formation of tectonic loading. Furthermore, the results for redox-sensitive elements (such as Mo, U, V and Ce) suggest that most areas of the NW Yangtze Block were probably in anoxic and even euxinic sedimentary environments during the depositional periods of the

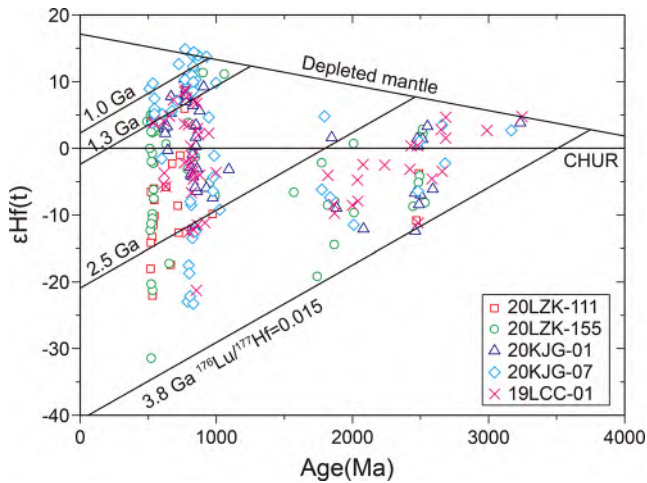


**Fig. 17.** Plot of  $\epsilon_{\text{Hf}}(t)$  v. U–Pb age (Ma) of the detrital zircons from the Canglangpu Formation sandstone samples of the Longzikou (samples 20LZK-111 and 20LZK-155) and Kangjiagou sections (samples 20KJG-01, 20KJG-07 and 19LCC-01). Grains with more than 10% discordance have been omitted. CHUR, chondritic uniform reservoir. The sloping parallel lines are two-stage Hf model age ( $T_{\text{DM2}}$ ).

Maidiping and Qiongzhusi formations, whereas the Canglangpu Formation strata were deposited in relatively oxic, shallow water environments (Fig. 13c). These interpretations are consistent with the variations in outcrop lithofacies (Fig. 5a). Furthermore, the obvious Ba enrichments in the Maidiping and Qiongzhusi formations (Figs 11, 13c and 14) reveal that the sedimentary environments were potentially influenced by hydrothermal events on the seafloor. Representative trace elements of the Longzikou section fine-grained sedimentary rocks reveal a possible continental arc source for the Early Cambrian deposits (Fig. 12). All the observations indicate a tectonic transition from a passive margin to an active orogenic setting in the NW Yangtze Block.

In addition, the regional seismic profile shows a typical foreland basin geometry that is considerably thickened in the NW and significantly thinned in the SE, consistent with the development of a foredeep in the NW and the development of an uplift in the SE for a foreland basin. An unconformity between the Ediacaran Dengying Formation and Lower Cambrian took place across the Yangtze Block (Gu *et al.* 2016a, b), implying a transition from a passive margin to an active foreland basin. The overall basin geometry indicates that the Lower Cambrian sequence was deposited in a foreland basin setting and sediments were derived from the northwestward uplifted terranes, such as the Jiaoziding complex, the Bikou terrane and the West Qinling orogen.

Detrital zircon age spectra have distinctive distribution patterns that reflect the tectonic setting of the basin in which they are deposited (Cawood *et al.* 2012). Some of the Lower Cambrian zircons display a euhedral, prismatic shape, suggesting that they are first-cycle detritus from a proximal source. Detrital zircons of the Canglangpu Formation within the Longmenshan have typical foreland basin-like age spectra. The ages of the youngest zircon grains of sediments are close to their depositional ages, together with older sources, indicating deposition in a convergent or collisional plate margin setting (Cawood *et al.* 2012). Hence, the dominant *c.* 530 Ma age signature of detrital zircons from the Longzikou samples may represent an important tectonomagmatic event that occurred to the west of the present-day Longmenshan fold–thrust belt. The foreland sediments were largely derived from elevated terranes (e.g. the Jiaoziding complex, the Bikou terrane and the West Qinling orogen) located to the west of the Longmenshan.

Therefore, we propose that an Early Cambrian continental arc assemblage and older continental crust were exposed to the NW,

and served as a potential source for the sediments deposited in the present-day Longmenshan fold–thrust belt and in the Sichuan Basin to the SE. These arcs are also probably now buried under the Songpan–Ganzi terrane, to the west of the Longmenshan. Our results suggest that an Early Cambrian foreland basin succession located in the Longmenshan and Sichuan Basin was the result of loading to the NW; for instance, in the Bikou terrane and the West Qinling orogen.

### Origin of the foreland basin and related orogeny

We suggest that an Early Cambrian foreland basin developed in the NW Yangtze Block was related to a lithospheric flexural loading to the west of the present-day Longmenshan fold–thrust belt. Moreover, the loading could be related to crustal thickening that resulted generally from oceanic plate subduction and subsequent arc–continent convergence and collision (Cant and Stockmal 1989; Ettensohn 1993). Thus, it is of great importance to determine the northwestern boundary of the Yangtze Block during Ediacaran to Cambrian times, and further to determine the distribution of adjacent oceans. The present-day northwestern boundary of the Sichuan Basin is the Longmenshan fold–thrust belt, and the boundary of the North China and South China cratons is the Mianlue suture. Because of the complex evolution history, the NW boundary of the Yangtze Block during the Ediacaran to Cambrian remains controversial, and the Longmenshan (Dong and Santosh 2016; Luo *et al.* 2018), the Bikou terrane (Yan *et al.* 2003, 2004; Druschke *et al.* 2006; Li *et al.* 2018; Gao *et al.* 2020) and the West Qinling orogen (Meng and Zhang 1999) have all been considered as boundaries. Whether the West Qinling orogen belonged to the Yangtze Block during that time remains controversial.

However, a large amount of evidence has demonstrated that during the Ediacaran to Cambrian, the boundary of the Yangtze Block was located along the Tianshui and Sangdan sutures. Hence, the Longmenshan fold–thrust belt, the Bikou terrane and the West Qinling orogen are thought to be closely related to the Yangtze Block during that time. Moreover, field investigations of the Tonian to Cryogenian in the West Qinling orogen reveal lithostratigraphic features similar to those of the Yangtze Block, but different from those of the North China Craton, especially the occurrence of the tillite in the Cryogenian. Hence, we favour the view that the West Qinling orogen was connected to the Yangtze Block during the Ediacaran to Cambrian.

Recently, large numbers of magmatic zircon ages have been reported along the Wushan, Tianshui and Sangdan sutures, which spread predominantly between 534 and 471 Ma (Dong *et al.* 2007, 2011; Pei *et al.* 2007a, b), indicating that a palaeo-ocean subduction event occurred during the Early Cambrian to Ordovician along the NW boundary of the Yangtze Block. The palaeo-ocean has been referred to as the Shangdan ocean (Dong *et al.* 2011) or Proto-Tethys ocean (Pei *et al.* 2007b; Li *et al.* 2018). There are two distinct viewpoints on the palaeo-ocean subduction polarity: a northward subduction (Dong *et al.* 2011) or southward subduction direction (Li *et al.* 2018). Although the subduction polarity of the Proto-Tethys ocean is beyond the range of this study, we prefer southward subduction because the microterranes underwent southward shift during the assembly of the Gondwana supercontinent (Li *et al.* 2018).

The widespread *c.* 530 Ma age of detrital zircons found in the Lower Cambrian sandstones from the Longmenshan fold–thrust belt is consistent with the age of arc magmatism located near the Proto-Tethys ocean suture. The ternary plots of La–Th–Sc and Th–Sc–Zr/10 for Lower Cambrian fine-grained sedimentary rocks of the Longzikou section also indicate the occurrence of continental arcs (Fig. 12). Recently, we have found records of the Early Cambrian magmatic event in the Longmenshan fold–thrust belt,

including a thick volcanoclastic rock sequence (more than hundreds of metres thick, *c.* 526 Ma) and gabbro intrusions (*c.* 528 Ma), which could be related to oceanic plate subduction. These imply that the continental arc rocks, which resulted from the Proto-Tethys ocean subduction, could be a potential source for the Lower Cambrian sediments in the Longmenshan and Sichuan Basin. The consequences of the Proto-Tethys ocean subduction include convergence and subsequent collision of microterranes, such as the present-day West Qinling orogen, the Bikou terrane and the Jiaoziding complex. We consider that these microterranes were elevated after *c.* 530 Ma, experienced exhumation and provided sediments to the SE. The clastic components in the Longmenshan are also consistent with the lithology of microterranes located to the west of the Longmenshan. The framework grain petrographic mode (QFL ternary plot) of Canglangpu Formation coarse-grained sandstones from the Kangjiagou section shows a recycled orogenic setting (Fig. 10a), indicative of orogeny occurring to the west. Therefore, the orogeny attributed to the Proto-Tethys ocean subduction produced a loading in the present-day West Qinling orogen and Bikou terrane, and a foreland basin in the Longmenshan and Sichuan Basin owing to lithospheric flexure.

Early Cambrian orogeny has been demonstrated to occur in the NW Yangtze Block. This period of orogeny, however, has not been defined by previous studies. Because of its importance for the tectonics of the Yangtze Block and its implications for gas exploration of the Sichuan Basin, an orogenic event name should

be coined. In this study, we would like to give a local orogenic name following previous rules, and refer to the Early Cambrian orogeny in the NW Yangtze Block as the Motianling orogeny, because of the extensive exposure and intense uplift of the Motianling region during that time.

In addition to loading, the geometry of a foreland basin is largely dependent on the strength of lithospheric elastic flexure (*i.e.*  $T_e$ ). The Sichuan Basin lithosphere is likely to have a high  $T_e$ . Previous researchers have given some representative values of  $T_e$ , most of which are around 50 km, implying a high- $T_e$  nature. Li *et al.* (2003) analysed the thickness variations of Triassic sedimentary rocks deposited in the foreland of the Longmenshan and estimated that  $T_e$  was 43–54 km. Jiang and Jin (2005) modelled profiles of Bouguer gravity anomalies to estimate  $T_e$  values close to 45 km for the Sichuan Basin in their preferred model of variable  $T_e$ . Fielding and McKenzie (2012) obtained a best-fit flexure model with  $T_e = 54.6$  km by virtue of the Watts (2001) broken model. Therefore, *c.* 50 km of  $T_e$  could be reasonable for the Sichuan Basin. If we apply the broken model and use 50 km of  $T_e$ , we can assign an orogenic loading at the Bikou terrane that would produce a downwarp in the Longmenshan and western Sichuan Basin and a peripheral bulge in the eastern Sichuan Basin, consistent with the basin geometry of the Early Cambrian as shown in Figure 4. Hence, the development of the foreland basin during the Early Cambrian time is reasonable from the viewpoint of lithospheric elastic flexure.

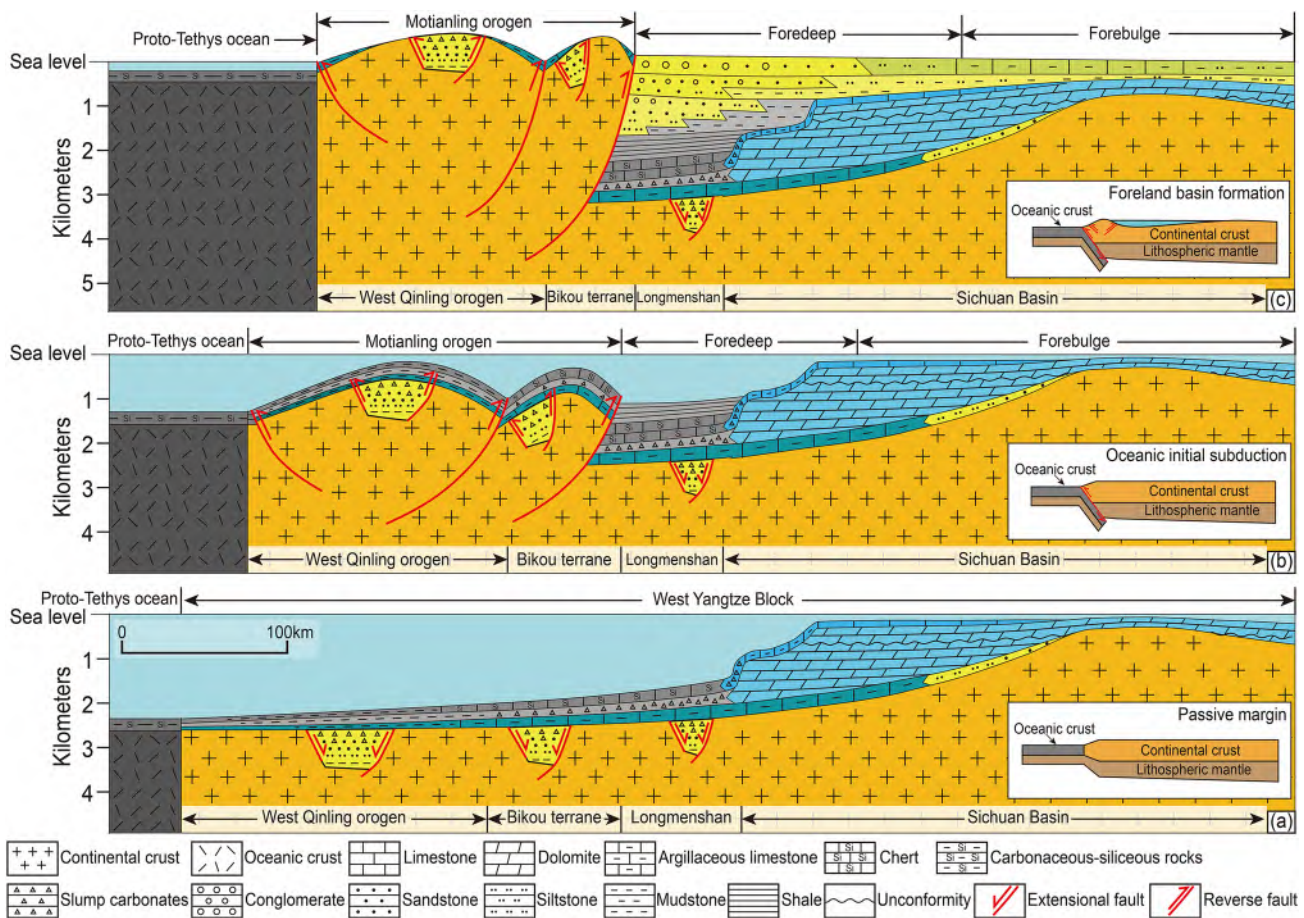


**Fig. 18.** Hypothetical schematic tectonic model illustrating the proposed transition from a passive margin in the Ediacaran to a foreland basin in the Early Cambrian in the NW Yangtze Block. Insets present the structure of oceanic and continental crust and the tectonic transition at lithospheric scale. (a) Passive margin stage during the Ediacaran. (b) Initiation of oceanic subduction during the Early Cambrian (*c.* 530 Ma) resulted in orogenic loading (Motianling orogen), flexural warping of the lithosphere and subsequent filling of the foredeep in the present-day Longmenshan fold-thrust belt and western Sichuan Basin. (c) As oceanic subduction continued, collisions and uplifts of microterranes provided sediments to the foredeep ahead of the advancing tectonic loading, and a peripheral bulge formed in the SE Sichuan Basin.

### Early Cambrian tectonic and sedimentary evolution in the NW Yangtze Block; implications and perspectives

In summary, a passive margin was formed during the Ediacaran and the beginning of the Early Cambrian, facing the Proto-Tethys ocean to the NW (Fig. 18a). In the Early Cambrian at *c.* 530 Ma, Proto-Tethys ocean subduction beneath the NW Yangtze Block was initiated, producing continental arcs along the NW margin of the Yangtze Block, and microterranes, such as the present-day West Qinling orogen and the Bikou terrane, were uplifted above sea level (Fig. 18b). As subduction continued, the convergence and collision of microterranes took place and the Motianling orogen was formed in the present-day West Qinling orogen, the Bikou terrane, the Jiaoziding complex and even in the Songpan–Ganzi terrane regions (Fig. 18c). The Motianling orogen not only resulted in loading to produce a downwarp in the Longmenshan area and western Sichuan Basin owing to lithospheric flexure, but also provided detritus to fill the foreland basin. Owing to the high strength of the Sichuan Basin lithosphere, a forebulge was formed in the eastern Sichuan Basin, consistent with the overall basin geometry. The reverse-graded succession of the Lower Cambrian, from shale to conglomerate, indicates the gradual advance of the Motianling orogen as subduction continued.

The recognition of the Early Cambrian foreland basin in the NW Yangtze Block can provide insight into the gas exploration of the Lower Cambrian in the Sichuan Basin. The foredeep areas have been demonstrated to be favourable for the accumulation of fine-grained hydrocarbon source rocks of the Lower Cambrian (e.g. Maidiping and Qiongzhusi formations), and the forebulge and associated palaeogeographical high areas would be favourable for widespread ooid deposition of the Lower Cambrian (e.g. Canglangpu and Longwangmiao formations). This study also has important implications for the assembly of East Gondwana during Late Neoproterozoic to Early Paleozoic times. It may be not necessary to link the western Yangtze Block, South China, with the other blocks. We note that previous investigations have given few reports of structural deformation, metamorphism and magmatic events during the Early Cambrian in the NW Yangtze Block. Thus, further work is required to verify the hypothesis in this study. Flexural modelling based on lithospheric strength and tectonic loading will be considered in our future research.

### Conclusions

The Ediacaran to Cambrian in the NW Yangtze Block has long been considered to have formed in a passive margin setting; however, the occurrence of Lower Cambrian thick clastic rocks has led us to think about their provenances and origin. Our results show that the northwestern Yangtze Block experienced a tectonic transition from a passive margin in the Ediacaran to a foreland basin in the Early Cambrian. A regional lithostratigraphic correlation across the Yangtze Block indicates a considerable strata absence from NW to SE, indicating that an orogeny might have taken place to the NW. A regional seismic profile across the Sichuan Basin shows a typical foreland basin geometry. The provenance analyses of the Lower Cambrian in the Longmenshan fold–thrust belt, including field-based sedimentology, sandstone petrography, geochemistry and detrital zircon U–Pb ages and Hf isotope study, indicate that the sediments were most probably derived from northwestern proximal terranes. The dominant *c.* 530 Ma age of detrital zircons with positive  $\varepsilon_{\text{Hf}}(t)$  values reveals that continental arcs served as proximal sediment sources. We propose that the formation of the Early Cambrian foreland basin was related to Proto-Tethys ocean subduction at *c.* 530 Ma and that subsequent collisions between arcs and microterranes resulted in orogenic loading.

**Acknowledgements** We would like to thank Baomin Zhang, Ping Luo, Wuling Mo, Ruizhi Liuzhu and Tong Lin from RIPED for their help during fieldwork in the Longmenshan. Xiaotian Shen, Hanjing Fu and Ling Wang from Xiamen University are thanked for their contributions to sample collection and laboratory analysis. The authors gratefully acknowledge constructive and precise reviews by Liang Qiu from China University of Geosciences (Beijing) and an anonymous reviewer, and valuable comments by Editor Renjie Zhou from The University of Queensland, which have considerably improved the quality of the paper.

**Author contributions** ZG: conceptualization (lead), formal analysis (equal), funding acquisition (lead), investigation (lead), methodology (equal), project administration (equal), writing – original draft (lead), writing – review & editing (equal); XJ: formal analysis (equal), methodology (equal), writing – original draft (supporting), writing – review & editing (equal); ABW: formal analysis (equal), methodology (equal), writing – review & editing (equal); XZ: formal analysis (equal), writing – original draft (supporting); GL: formal analysis (equal), investigation (supporting); HJ: formal analysis (equal)

**Funding** This study was supported by the National Petroleum Project of China (no. 2016ZX05004005-001) and the Science and Technology Project of PetroChina (nos 2021DJ0501, kt2020-01-03 and 2022KT0101).

**Competing interests** The authors declare that they have no known competing financial interests or personal relationships that could have appeared to influence the work reported in this paper.

**Data availability** All data generated or analysed during this study are included in this published article (and its supplementary information files).

*Scientific editing by Renjie Zhou*

### References

- Andersen, T. 2002. Correction of common lead in U–Pb analyses that do not report  $^{204}\text{Pb}$ . *Chemical Geology*, **192**, 59–79, [https://doi.org/10.1016/S0009-2541\(02\)00195-X](https://doi.org/10.1016/S0009-2541(02)00195-X)
- Belousova, E.A., Kostitsyn, Y.A., Griffin, W.L., Begg, G.C., O'Reilly, S.Y. and Pearson, N.J. 2010. The growth of the continental crust: constraints from zircon Hf-isotope data. *Lithos*, **119**, 457–466, <https://doi.org/10.1016/j.lithos.2010.07.024>
- Bhatia, M.R. and Crook, K.A. 1986. Trace element characteristics of graywackes and tectonic setting discrimination of sedimentary basins. *Contributions to Mineralogy and Petrology*, **92**, 181–193, <https://doi.org/10.1007/BF00375292>
- Bird, J.M. and Dewey, J.F. 1970. Lithosphere plate–continental margin tectonics and the evolution of the Appalachian orogeny. *Geological Society of America Bulletin*, **81**, 1031–1060, [https://doi.org/10.1130/0016-7606\(1970\)81\[1031:LPMTAT\]2.0.CO;2](https://doi.org/10.1130/0016-7606(1970)81[1031:LPMTAT]2.0.CO;2)
- Blichert-Toft, J. and Albarède, F. 1997. The Lu–Hf isotope geochemistry of chondrites and the evolution of the mantle–crust system. *Earth and Planetary Science Letters*, **148**, 243–258, [https://doi.org/10.1016/S0012-821X\(97\)00040-X](https://doi.org/10.1016/S0012-821X(97)00040-X)
- Bradley, D.C. 2008. Passive margins through earth history. *Earth-Science Reviews*, **91**, 1–26, <https://doi.org/10.1016/j.earscirev.2008.08.001>
- Bradley, D.C. and Kusky, T.M. 1986. Geologic evidence for rate of plate convergence during the Taconic arc–continent collision. *Journal of Geology*, **94**, 667–681, <https://doi.org/10.1086/629073>
- Cant, D.J. and Stockmal, G.S. 1989. The Albert foreland basin: relationship between stratigraphy and Cordilleran terrane-accretion events. *Canadian Journal of Earth Sciences*, **26**, 1964–1975, <https://doi.org/10.1139/e89-166>
- Cawood, P.A., Hawkesworth, C.J. and Dhuime, B. 2012. Detrital zircon record and tectonic setting. *Geology*, **40**, 875–878, <https://doi.org/10.1130/G32945.1>
- Chang, E.Z. 2010. Geology and tectonics of the Songpan–Ganzi fold belt, southwestern China. *International Geology Review*, **42**, 813–831, <https://doi.org/10.1080/00206810009465113>
- Charvet, J., Shu, L.S., Faure, M., Choulet, F., Wang, B., Lu, H.F. and Breton, N.L. 2010. Structural development of the Lower Paleozoic belt of South China: genesis of an intracontinental orogeny. *Journal of Asian Earth Sciences*, **39**, 309–330, <https://doi.org/10.1016/j.jseas.2010.03.006>
- Chen, Q., Sun, M., Long, X.P., Zhao, G.C. and Yuan, C. 2016. U–Pb ages and Hf isotopic record of zircons from the late Neoproterozoic and Silurian–Devonian sedimentary rocks of the western Yangtze Block: implications for its tectonic evolution and continental affinity. *Gondwana Research*, **31**, 184–199, <https://doi.org/10.1016/j.gr.2015.01.009>
- Chen, Q., Sun, M., Long, X.P., Zhao, G.C., Wang, J., Yu, Y. and Yuan, C. 2018. Provenance study for the Paleozoic sedimentary rocks from the west Yangtze Block: constraint on possible link of South China to the Gondwana supercontinent reconstruction. *Precambrian Research*, **309**, 271–289, <https://doi.org/10.1016/j.precamres.2017.01.022>

- Chen, S.F. and Wilson, C.J.L. 1996. Emplacement of the Longmen Shan Thrust–Nappe Belt along the eastern margin of the Tibetan Plateau. *Journal of Structural Geology*, **18**, 413–430, [https://doi.org/10.1016/0191-8141\(95\)00096-V](https://doi.org/10.1016/0191-8141(95)00096-V)
- Chen, S.F., Wilson, C.J.L. and Worley, B.A. 1995. Tectonic transition from the Songpan–Ganze Fold Belt to the Sichuan Basin, south-western China. *Basin Research*, **7**, 235–253, <https://doi.org/10.1111/j.1365-2117.1995.tb00108.x>
- Chen, Y.L. and Yang, Z.F. 2000. Nd model ages of sedimentary profile from the northwest Yangtze Craton, Guangyuan, Sichuan province, China and their geological implication. *Geochemical Journal*, **34**, 263–270, <https://doi.org/10.2343/geochemj.34.263>
- Cohen, C.R. 1982. Model for a passive to active continental margin transition: implications for hydrocarbon exploration. *AAPG Bulletin*, **66**, 708–718.
- Cooper, M., Weissenberger, J. et al. 2001. Basin evolution in western Newfoundland: new insights from hydrocarbon exploration. *AAPG Bulletin*, **85**, 393–418, [https://doi.org/10.1306/8626C901-173B-11D7-8645000\\_02C1865D](https://doi.org/10.1306/8626C901-173B-11D7-8645000_02C1865D)
- Dewey, J.F. 1969a. Evolution of the Appalachian/Caledonian orogen. *Nature*, **222**, 124–129, <https://doi.org/10.1038/222124a0>
- Dewey, J.F. 1969b. Continental margins: a model for conversion of Atlantic type to Andean type. *Earth and Planetary Science Letters*, **6**, 189–197, [https://doi.org/10.1016/0012-821X\(69\)90089-2](https://doi.org/10.1016/0012-821X(69)90089-2)
- Dewey, J.F. 1971. A model for the Lower Palaeozoic evolution of the southern margin of the early Caledonides of Scotland and Ireland. *Scottish Journal of Geology*, **7**, 219–240, <https://doi.org/10.1144/sjg07030219>
- Dewey, J. and Mange, M. 1999. Petrography of Ordovician and Silurian sediments in the western Irish Caledonides: tracers of a short-lived Ordovician continent–arc collision orogeny and the evolution of the Laurentian Appalachian–Caledonian margin. *Geological Society, London, Special Publications*, **164**, 55–107, <https://doi.org/10.1144/GSL.SP.1999.164.01.05>
- Dickinson, W.R. 1985. Interpreting provenance relations from detrital modes of sandstones. In: Zuffa, G.G. (ed.) *Provenance of Arenites*. Springer, 333–361.
- Domeier, M. 2018. Early Paleozoic tectonics of Asia: towards a full-plate model. *Geoscience Frontiers*, **9**, 789–862, <https://doi.org/10.1016/j.gsf.2017.11.012>
- Dong, Y.P. and Santosh, M. 2016. Tectonic architecture and multiple orogeny of the Qinling Orogenic Belt, Central China. *Gondwana Research*, **29**, 1–40, <https://doi.org/10.1016/j.gr.2015.06.009>
- Dong, Y.P., Zhang, G.W., Yang, Z., Zhao, X., Ma, H.Y. and Yao, A.P. 2007. Geochemistry of the E-MORB type ophiolite and related volcanic rocks from the Wushan area, West Qinling. *Science in China (Series D: Earth Sciences)*, **50**, 234–245, <https://doi.org/10.1007/s11430-007-6004-3>
- Dong, Y.P., Liu, X.M., Santosh, M., Zhang, X.N., Chen, Q., Zhang, C. and Zhang, Z. 2011. Neoproterozoic subduction tectonics of the northwestern Yangtze Block in South China: constraints from zircon U–Pb geochronology and geochemistry of mafic intrusions in the Hannan Massif. *Precambrian Research*, **189**, 66–90, <https://doi.org/10.1016/j.precamres.2011.05.002>
- Dong, Y.P., Zhang, X.N. et al. 2015. Propagation tectonics and multiple accretionary processes of the Qinling Orogen. *Journal of Asian Earth Sciences*, **104**, 84–98, <https://doi.org/10.1016/j.jseas.2014.10.007>
- Dong, Y.P., Sun, S.S. et al. 2017. Neoproterozoic subduction–accretionary tectonics of the South Qinling Belt, China. *Precambrian Research*, **293**, 73–90, <https://doi.org/10.1016/j.precamres.2017.02.015>
- Druschke, P., Hanson, A.D., Yan, Q.R., Wang, Z.Q. and Wang, T. 2006. Stratigraphic and U–Pb SHRIMP detrital zircon evidence for a Neoproterozoic continental arc, central China: Rodinia implications. *The Journal of Geology*, **114**, 627–636, <https://doi.org/10.1086/506162>
- Ettensohn, F.R. 1993. Possible flexural controls on the origins of extensive, ooid-rich, carbonate environments in the Mississippian of the United States. *AAPG Studies in Geology*, **35**, 13–30.
- Fielding, E.J. and McKenzie, D. 2012. Lithospheric flexure in the Sichuan Basin and Longmen Shan at the eastern edge of Tibet. *Geophysical Research Letters*, **39**, L09311, <https://doi.org/10.1029/2012GL051680>
- Floyd, P.A. and Leveridge, B.E. 1987. Tectonic environment of the Devonian Gramscatho basin, south Cornwall: framework mode and geochemical evidence from turbiditic sandstones. *Journal of the Geological Society, London*, **144**, 531–542, <https://doi.org/10.1144/gsjgs.144.4.0531>
- Gao, F., Pei, X.Z. et al. 2020. Provenance and depositional mechanism analyses of the Yangtze Formation, northwestern margin of the Yangtze Block, southwestern China. *Journal of Geodynamics*, **138**, 101750, <https://doi.org/10.1016/j.jog.2020.101750>
- Gbadayan, R. and Dix, G.R. 2013. The role of regional and local structure in a Late Ordovician (Edenian) foreland platform-to-basin succession inboard of the Taconic Orogen, Central Canada. *Geosciences*, **3**, 216–239, <https://doi.org/10.3390/geosciences3020216>
- Griffin, W.L., Belousova, E.A., Shee, S.R., Pearson, N.J., and O'Reilly, S.Y. 2004. Archean crustal evolution in the northern Yilgarn Craton: U–Pb and Hf-isotope evidence from detrital zircons. *Precambrian Research*, **131**, 231–282, <https://doi.org/10.1016/j.precamres.2003.12.011>
- Gu, Z.D., Yin, J.F. et al. 2016a. Tectonic evolution from Late Sinian to Early Paleozoic and natural gas exploration in northwestern Sichuan Basin, SW China. *Petroleum Exploration and Development*, **43**, 1–12, [https://doi.org/10.1016/S1876-3804\(16\)30001-5](https://doi.org/10.1016/S1876-3804(16)30001-5)
- Gu, Z.D., Yin, J.F. et al. 2016b. Discovery of Xuanhan–Kaijiang paleo uplift and its significance in the Sichuan Basin, SW China. *Petroleum Exploration and Development*, **43**, 976–987, [https://doi.org/10.1016/S1876-3804\(16\)30115-X](https://doi.org/10.1016/S1876-3804(16)30115-X)
- Gu, Z.D., Lonergan, L., Zhai, X.F., Zhang, B.M. and Lu, W.H. 2021. The formation of the Sichuan Basin, South China, during the Late Ediacaran to Early Cambrian. *Basin Research*, **33**, 12559, <https://doi.org/10.1111/bre.12559>
- Gutschick, R.C. and Sandberg, C.A. 1983. Mississippian continental margins of the conterminous United States. *SEPM Special Publications*, **33**, 79–96.
- Hiscott, R.N. 1978. Provenance of Ordovician deep-water sandstones, Tourelle Formation, Quebec, and implications for initiation of the Taconic orogeny. *Canadian Journal of Earth Sciences*, **15**, 1579–1597, <https://doi.org/10.1139/e78-163>
- Houseknecht, D.W. 1986. Evolution from passive margin to foreland Basin: the Atoka Formation of the Arkoma Basin, South-Central U.S.A. In: Allen, P.A. and Homewood, P. (eds) *Foreland Basins*. Blackwell Scientific, Oxford, 327–346.
- Hui, B., Dong, Y.P., Zhang, F.F., Sun, S.S. and He, S. 2020. Neoproterozoic active margin in the northwestern Yangtze Block, South China: new clues from detrital zircon U–Pb geochronology and geochemistry of sedimentary rocks from the Hengdan Group. *Geological Magazine*, **158**, <https://doi.org/10.1017/S0016756820000898>
- Hui, B., Dong, Y.P., Zhang, F.F., Sun, S.S. and He, S. 2021. Petrogenesis and tectonic implications of the Neoproterozoic mafic intrusions in the Bikou Terrane along the northwestern margin of the Yangtze Block, South China. *Ore Geology Reviews*, **131**, 104014, <https://doi.org/10.1016/j.oregeorev.2021.104014>
- Jacobi, R.D. 1981. Peripheral bulge – a causal mechanism for the Lower/Middle Ordovician unconformity along the western margin of the Northern Appalachians. *Earth and Planetary Science Letters*, **56**, 245–251, [https://doi.org/10.1016/0012-821X\(81\)90131-X](https://doi.org/10.1016/0012-821X(81)90131-X)
- Jia, D., Wei, G.Q., Chen, Z.X., Li, B.L., Zeng, Q. and Yang, G. 2006. Longmen Shan fold–thrust belt and its relation to the western Sichuan Basin in central China: new insights from hydrocarbon exploration. *AAPG Bulletin*, **90**, 1425–1447, <https://doi.org/10.1306/03230605076>
- Jian, X., Guan, P., Zhang, D.W., Zhang, W., Feng, F., Liu, R.J. and Lin, S.D. 2013. Provenance of Tertiary sandstone in the northern Qaidam basin, northeastern Tibetan Plateau: integration of framework petrography, heavy mineral analysis and mineral chemistry. *Sedimentary Geology*, **290**, 109–125, <https://doi.org/10.1016/j.sedgeo.2013.03.010>
- Jian, X., Zhang, W., Yang, S. and Kao, S.J. 2020. Climate-dependent sediment composition and transport of mountainous rivers in tectonically stable, subtropical East Asia. *Geophysical Research Letters*, **47**, e2019GL086150, <https://doi.org/10.1029/2019GL086150>
- Jiang, Q.G. 1994. Sedimentary environment analysing of rocks in Taiyangding Group, Cambrian–Ordovician systems, the northern part of Ruogai, Sichuan. *Journal of Changchun University of Earth Sciences*, **24**, 272–277 [in Chinese with English abstract].
- Jiang, G.Q., Shi, X.Y., Zhang, S.H., Wang, Y. and Xiao, S.H. 2011. Stratigraphy and paleogeography of the Ediacaran Doushantuo Formation (c. 635–551 Ma) in South China. *Gondwana Research*, **19**, 831–849, <https://doi.org/10.1016/j.gr.2011.01.006>
- Jiang, X.D. and Jin, Y. 2005. Mapping the deep lithospheric structure beneath the eastern margin of the Tibetan Plateau from gravity anomalies. *Journal of Geophysical Research*, **110**, B07407, <https://doi.org/10.1029/2004JB003394>
- Karabinos, P., Samson, S.D., Hepburn, J.C. and Stoll, H.M. 1998. Taconian orogeny in the New England Appalachians: collision between Laurentia and the Shelburne Falls arc. *Geology*, **26**, 215–218, [https://doi.org/10.1130/0091-7613\(1998\)026<0215:TOITNE>2.3.CO;2](https://doi.org/10.1130/0091-7613(1998)026<0215:TOITNE>2.3.CO;2)
- Li, H.B., Jia, D., Wu, L., Zhang, Y., Yin, H.W., Wei, G.Q., and Li, B.L. 2013. Detrital zircon provenance of the Lower Yangtze foreland basin deposits: constraints on the evolution of the early Paleozoic Wuyi–Yunkai orogenic belt in South China. *Geological Magazine*, **150**, 959–974, <https://doi.org/10.1017/S0016756812000969>
- Li, J.Y., Wang, X.L. and Gu, Z.D. 2018. Early Neoproterozoic arc magmatism of the Tongmuliang Group on the northwestern margin of the Yangtze Block: implications for Rodinia Assembly. *Precambrian Research*, **309**, 181–197, <https://doi.org/10.1016/j.precamres.2017.04.040>
- Li, W., Yu, H.Q. and Deng, H.B. 2012. Stratigraphic division and correlation and sedimentary characteristics of the Cambrian in central–southern Sichuan Basin. *Petroleum Exploration and Development*, **39**, 725–735, [https://doi.org/10.1016/S1876-3804\(12\)60097-4](https://doi.org/10.1016/S1876-3804(12)60097-4)
- Li, Y., Allen, P.A., Densmore, A.L. and Qiang, X. 2003. Evolution of the Longmen Shan foreland basin (western Sichuan, China) during the Late Triassic Indosinian Orogeny. *Basin Research*, **15**, 117–138, <https://doi.org/10.1046/j.1365-2117.2003.00197.x>
- Li, Y.F., Lai, S.C., Qin, J.F., Liu, X. and Wang, J. 2007. Geochemical characteristics of Bikou volcanic group and Sr–Nd–Pb isotopic composition: evidence for breakup event in the north margin of Yangtze plate, Jining era. *Science in China (Series D: Earth Sciences)*, **50**, 339–350, <https://doi.org/10.1007/s11430-007-6007-0>
- Li, Y.M. 1991. A discussion about the time, sequence, and ore-forming characteristic of Bikou Group in the south of Gansu province. *Gansu Geology*, **12**, 38–69 [in Chinese with English abstract].
- Li, Z.X., Li, X.H., Wartho, J.A., Clark, C., Li, W.X., Zhang, C.L. and Bao, C.M. 2010. Magmatic and metamorphic events during the early Paleozoic Wuyi–Yunkai orogeny, southeastern South China: new age constraints and pressure–

- temperature conditions. *Geological Society of America Bulletin*, **122**, 772–793, <https://doi.org/10.1130/B30021.1>
- Liu, J.J., Liu, J.M. et al. 1998. Judging the sedimentary environment of the chert formation on the chemical characteristics of rocks in western Qinling Mountains. *Acta Sedimentologica Sinica*, **20**, 43–49 [in Chinese with English abstract].
- Liu, J.J., Feng, C.X., Liu, J.M., Zheng, M.H. and Li, C.Y. 2004. Reidentification of the ore-hosted strata age and metallogenic age of the strata bound Au–Se deposits, the western Qinling mountains. *Earth Science Frontiers (China University of Geosciences, Beijing)*, **11**, 435–443 [in Chinese with English abstract].
- Liu, S.F. and Zhang, G.W. 1999. Process of rifting and collision along plate margins of the Qinling orogenic belt and its geodynamics. *Acta Geologica Sinica*, **73**, 275–288, <https://doi.org/10.1111/j.1755-6724.1999.tb00836.x>
- Ludwig, K.R. 2003. ISOPLOT 3: a geochronological toolkit for Microsoft excel. *Berkeley Geochronology Centre Special Publications*, **4**, 74.
- Luo, B.J., Liu, R. et al. 2018. Neoproterozoic continental back-arc rift development in the Northwestern Yangtze Block: evidence from the Hannan intrusive magmatism. *Gondwana Research*, **59**, 27–42, <https://doi.org/10.1016/j.gr.2018.03.012>
- Mange, M.A. and Maurer, H.F.W. 1992. *Heavy Minerals in Colour*. Chapman and Hall, London.
- Mao, F., Pei, X.Z. et al. 2021. The LA-ICP-MS U–Pb dating of detrital zircons from the Nanhua System in Bikou Terrane, northwestern margin of Yangtze Block. *Sedimentary Geology and Tethyan Geology*, **41**, 41–57 [in Chinese in English abstract], <https://doi.org/10.1016/j.cnki.1009-3850.2020.10009>
- Mattauer, M., Matte, P. et al. 1985. Tectonics of the Qinling Belt: build-up and evolution of eastern Asia. *Nature*, **317**, 496–500, <https://doi.org/10.1038/317496a0>
- McKerrow, W.S., Niocaill, C.A. and Dewey, J.F. 2000. The Caledonian Orogeny redefined. *Journal of the Geological Society, London*, **157**, 1149–1154, <https://doi.org/10.1144/jgs.157.6.1149>
- McLennan, S.M., Hemming, S., McDaniel, D.K. and Hanson, G.N. 1993. Geochemical approaches to sedimentation, provenance, and tectonics. In: Johnsson, M.J. and Basu, A. (eds) *Processes Controlling the Composition of Clastic Sediments*. Geological Society of America Special Paper, **284**, 21–40, <https://doi.org/10.1130/SPE284-p21>
- Meng, Q.R. and Zhang, G.W. 1999. Timing of collision of the North and South China blocks: controversy and reconciliation. *Geology*, **27**, 123–126, [https://doi.org/10.1130/0091-7613\(1999\)027<0123:TOCOTN>2.3.CO;2](https://doi.org/10.1130/0091-7613(1999)027<0123:TOCOTN>2.3.CO;2)
- Pei, X.Z., Ding, S.P., Hu, B., Li, Y., Zhang, G.W. and Guo, J.F. 2004. Definition of the Guanzhizhen ophiolite in Tianshui area, western Qinling, and its geological significance. *Geological Bulletin of China*, **23**, 1202–1208 [in Chinese with English abstract].
- Pei, X.Z., Li, Z.C. et al. 2007a. Geochemical characteristics and zircon U–Pb isotopic ages of island-arc basic igneous complexes from the Tianshui area in West Qinling. *Frontiers of Earth Science in China*, **1**, 49–59, <https://doi.org/10.1007/s11707-007-0008-3>
- Pei, X.Z., Ding, S.P. and Zhang, G.W. 2007b. The LA-ICP-MS zircon U–Pb ages and geochemistry of the Baihua basic igneous complexes in Tianshui area of West Qinling. *Science in China (Series D: Earth Sciences)*, **50**, 264–276, <https://doi.org/10.1007/s11430-007-6028-8>
- Pei, X.Z., Ding, S.P. et al. 2007c. LA-ICP-MS zircon U–Pb dating of the gabbro from the Guanzhizhen ophiolite in the northern margin of the western Qinling and its geological significance. *Acta Geologica Sinica*, **81**, 1550–1561 [in Chinese with English abstract].
- Pei, X.Z., Ding, S.P. et al. 2009. Early Paleozoic Tianshui–Wushan tectonic zone of the northern margin of West Qinling and its tectonic evolution. *Acta Geologica Sinica*, **83**, 1547–1564 [in Chinese with English abstract].
- Pigram, C.J., Davies, P.J., Feary, D.A. and Symonds, P.A. 1989. Tectonic controls on carbonate platform evolution in southern Papua New Guinea: passive margin to foreland basin. *Geology*, **17**, 199–202, [https://doi.org/10.1130/0091-7613\(1989\)017<0199:TCOCP>2.3.CO;2](https://doi.org/10.1130/0091-7613(1989)017<0199:TCOCP>2.3.CO;2)
- Qin, K.L., Zhou, X.H. and He, S.P. 1990. The sequence and age division of Bikou Group in Motianling region bounded by Shaanxi, Gansu and Sichuan, China. *Bulletin of the Xi'an Institute of Geology and Mineral Resources, Chinese Academy of Geological Science*, **30**, 1–60 [in Chinese with English abstract].
- Read, J.F. 1980. Carbonate ramp-to-basin transitions and foreland basin evolution, Middle Ordovician, Virginia Appalachians. *AAPG Bulletin*, **64**, 1575–1612.
- Read, J.F. 1982. Carbonate platforms of passive (extensional) continental margins: types, characteristics and evolution. *Tectonophysics*, **81**, 195–212, [https://doi.org/10.1016/0040-1951\(82\)90129-9](https://doi.org/10.1016/0040-1951(82)90129-9)
- Read, J.F. and Repetski, J.E. 2012. Cambrian–lower Middle Ordovician passive carbonate margin, southern Appalachians. *AAPG Memoirs*, **98**, 357–382.
- Robertson, A.H.F. 1987a. The transition from a passive margin to an Upper Cretaceous foreland basin related to ophiolite emplacement in the Oman Mountains. *Geological Society of America Bulletin*, **99**, 633–653.
- Robertson, A.H.F. 1987b. Upper Cretaceous Muti Formation: transition of a Mesozoic nate platform to a foreland basin in the Oman Mountains. *Sedimentology*, **34**, 1123–1142.
- Shu, L.S., Jahn, B.M., Charvet, J., Santosh, M., Wang, B., Xu, X.S. and Jiang, S.Y. 2014. Early Paleozoic depositional environment and intraplate tectonism in the Cathaysia Block (South China): evidence from stratigraphic, structural, geochemical and geochronological investigations. *American Journal of Science*, **314**, 154–186, <https://doi.org/10.2475/01.2014.05>
- Sinha, A.K., Thomas, W.A., Hatcher, R.D. and Harrison, T.M. 2012. Geodynamic evolution of the central Appalachian orogeny: geochronology and compositional diversity of magmatism from Ordovician through Devonian. *American Journal of Science*, **312**, 907–966, <https://doi.org/10.2475/08.2012.03>
- Soderlund, U., Patchett, P.J., Vervoort, J.D. and Isachsen, C.E. 2004. The <sup>176</sup>Lu decay constant determined by Lu–Hf and U–Pb isotope systematics of Precambrian mafic intrusions. *Earth and Planetary Science Letters*, **219**, 311–324, [https://doi.org/10.1016/S0012-821X\(04\)00012-3](https://doi.org/10.1016/S0012-821X(04)00012-3)
- Song, W.H. 1987. Some new knowledge of Caledonian paleo-uplift in Sichuan Basin. *Natural Gas Industry*, **7**, 6–11 [in Chinese in English abstract].
- Song, W.H. 1996. Research on reservoir-formed conditions of large–medium gas fields of Leshan–Longnusi Palaeohigh. *Natural Gas Industry*, **16**, 13–26.
- Speed, R.C. and Sleep, N.H. 1982. Antler orogeny and foreland basin: a model. *Geological Society of America Bulletin*, **93**, 815–828, [https://doi.org/10.1130/0016-7606\(1982\)93<815:AOAFBA>2.0.CO;2](https://doi.org/10.1130/0016-7606(1982)93<815:AOAFBA>2.0.CO;2)
- Stockmal, G.S., Beaumont, C. and Boutillier, R. 1986. Geodynamic models of convergent margin tectonics: transition from rifted margin to overthrust belt and consequences for foreland-basin development. *AAPG Bulletin*, **70**, 181–190
- Taylor, S.R. and McLennan, S.M. 1985. *The Continental Crust: Its Composition and Evolution*. Blackwell Scientific Publications, Boston, 1–312.
- Thomas, W.A. 1983. Continental margins, orogenic belts, and intracratonic structures. *Geology*, **11**, 270–272, [https://doi.org/10.1130/0091-7613\(1983\)11<270:CMOBAI>2.0.CO;2](https://doi.org/10.1130/0091-7613(1983)11<270:CMOBAI>2.0.CO;2)
- Walker, K.R., Shanmugam, G. and Ruppel, S.C. 1983. A model for carbonate to terrigenous clastic sequences. *Geological Society of America Bulletin*, **94**, 700–712, [https://doi.org/10.1130/0016-7606\(1983\)94<700:AMFCTT>2.0.CO;2](https://doi.org/10.1130/0016-7606(1983)94<700:AMFCTT>2.0.CO;2)
- Wang, E.C., Meng, K. et al. 2014. Block rotation: tectonic response of the Sichuan basin to the southeastward growth of the Tibetan Plateau along the Xianshuihe–Xiaojiang fault. *Tectonics*, **33**, 686–717, <https://doi.org/10.1002/2013TC003337>
- Wang, J. and Li, Z.X. 2003. History of Neoproterozoic rift basins in South China: implications for Rodinia break-up. *Precambrian Research*, **122**, 141–158, [https://doi.org/10.1016/S0301-9268\(02\)00209-7](https://doi.org/10.1016/S0301-9268(02)00209-7)
- Wang, X.C., Li, X.H. et al. 2008. The Bikou basalts in the northwestern Yangtze block, South China: remnants of 820–810 Ma continental flood basalts? *Geological Society of America Bulletin*, **120**, 1478–1492, <https://doi.org/10.1130/B26310.1>
- Wang, Y.J., Zhang, F.F., Fan, W.M., Zhang, G.W., Chen, S.Y., Cawood, P.A. and Zhang, A.M. 2010. Tectonic setting of the South China Block in the early Paleozoic: resolving intracontinental and ocean closure models from detrital zircon U–Pb geochronology. *Tectonics*, **29**, TC6020, <https://doi.org/10.1029/2010TC002750>
- Watts, A.B. 2001. *Isostasy and Flexure of the Lithosphere*. Cambridge University Press, Cambridge.
- Wickstrom, L.M. and Stephens, M.B. 2020. Tonian–Cryogenian rifting and Cambrian–Early Devonian platformal to foreland basin development outside the Caledonide orogen. *Geological Society, London, Memoirs*, **50**, 451–477, <https://doi.org/10.1144/M50-2016-31>
- Xue, Z.H., Martelet, G. et al. 2017. Mesozoic crustal thickening of the Longmenshan belt (NE Tibet, China) by imbrication of basement slices: insights from structural analysis, petrofabric and magnetic fabric studies, and gravity modeling. *Tectonics*, **36**, 3110–3134, <https://doi.org/10.1002/2017TC004754>
- Yan, D.P., Qiu, L. et al. 2018a. Structural and geochronological constraints on the early Mesozoic north Longmen Shan Thrust Belt: foreland fold–thrust propagation of the SW Qinling orogenic belt, northeastern Tibetan plateau. *Tectonics*, **37**, 4595–4624, <https://doi.org/10.1029/2018TC004986>
- Yan, D.P., Zhou, Y., Qiu, L., Wells, M.L., Mu, H.X. and Xu, C.G. 2018b. The Longmenshan Tectonic Complex and adjacent tectonic units in the eastern margin of the Tibetan Plateau: a review. *Journal of Asian Earth Sciences*, **164**, 33–57, <https://doi.org/10.1016/j.jseae.2018.06.017>
- Yan, Q., Hanson, A.D. et al. 2004. Neoproterozoic subduction and rifting on the northern margin of the Yangtze Plate, China: implications for Rodinia reconstruction. *International Geological Review*, **46**, 817–832, <https://doi.org/10.2747/0020-6814.46.9.817>
- Yan, Q.R., Wang, Z.Q. et al. 2003. SHRIMP age and geochemistry of the Bikou volcanic terrane: implications for Neoproterozoic tectonics on the northern margin of the Yangtze Craton. *Acta Geologica Sinica*, **77**, 479–490, <https://doi.org/10.1111/j.1755-6724.2003.tb00128.x>
- Yang, L.M., Song, S.G., Allen, M.B., Su, L., Dong, J.L. and Wang, C. 2018. Oceanic accretionary belt in the West Qinling Orogen: links between the Qinling and Qilian orogens, China. *Gondwana Research*, **64**, 137–162, <https://doi.org/10.1016/j.gr.2018.06.009>
- Yao, W.H., Li, Z.X., Li, W.X., Li, X.H. and Yang, J.H. 2014. From Rodinia to Gondwanaland: a tale of detrital zircon provenance analyses from the southern Nanhua Basin, South China. *American Journal of Science*, **314**, 278–313, <https://doi.org/10.2475/01.2014.08>
- Ye, F.R., Li, Y.D. and Cui, Z.G. 1994. Understanding of the Taiyangding Group in Laerma district of Gansu, China. *Acta Geologica Gansu*, **3**, 27–30 [in Chinese with English abstract].
- Ye, T.Z., Huang, C.K. and Deng, Z.Q. 2017. Spatial database of 1:2 500 000 digital geologic map of People's Republic of China. *Geology in China*, **44**, 19–24 [in

- Chinese with English abstract], <https://doi.org/10.23650/data.H.2017.NGA121474.K1.1.1>
- Zhang, G.W., Meng, Q.R. and Lai, S.C. 1995. Tectonics and structure of Qinling orogenic belt. *Science in China (Series B)*, **38**, 1379–1394.
- Zhang, G.W., Meng, Q.R. and Yu, Z.P. 1996. Orogenic processes and dynamics of the Qinling. *Science in China (Series D)*, **39**, 225–234.
- Zhang, H.F., Zhang, L., Harris, N., Jin, L.L. and Yuan, H.L. 2006. U–Pb zircon ages, geochemical and isotopic compositions of granitoids in Songpan–Garze fold belt, eastern Tibetan Plateau: constraints on petrogenesis and tectonic evolution of the basement. *Contributions to Mineralogy and Petrology*, **152**, 75–88, <https://doi.org/10.1007/s00410-006-0095-2>
- Zhang, L.L., Zhu, D.C., Wang, Q., Zhao, Z.D., Liu, D. and Xie, J.C. 2019. Late Cretaceous volcanic rocks in the Sangri area, southern Lhasa Terrane, Tibet: evidence for oceanic ridge subduction. *Lithos*, **326–327**, 144–157, <https://doi.org/10.1016/j.lithos.2018.12.023>
- Zhang, Z.Q., Zhang, G.W., Tang, S.S. and Wang, J.H. 2001. On the age of metamorphic rocks of the Yudongzi Group and the Archean crystalline basement of the Qinling orogen. *Acta Geologica Sinica*, **75**, 198–204 [in Chinese with English abstract].
- Zhao, G.C. and Cawood, P.A. 2012. Precambrian geology of China. *Precambrian Research*, **222–223**, 13–54, <https://doi.org/10.1016/j.precamres.2012.09.017>
- Zhao, X.S., Ma, S.L., Zou, X.H. and Xiu, Z.L. 1990. The study of the age, sequence, volcanism and mineralization of Bikou Group in Qinling–Dabashan. *Bulletin of the Xi'an Institute of Geological Mineral Resources, Chinese Academy of Geological Science*, **30**, 1–60 [in Chinese with English abstract].
- Zheng, J.P., Griffin, W.L. *et al.* 2010. Tectonic affinity of the west Qinling terrane (central China): north China or Yangtze? *Tectonics*, **29**, TC2009, <https://doi.org/10.1029/2008TC002428>
- Zhou, C.M. and Xiao, S.H. 2007. Ediacaran  $\delta^{13}\text{C}$  chemostratigraphy of South China. *Chemical Geology*, **237**, 89–108, <https://doi.org/10.1016/j.chemgeo.2006.06.021>
- Zhou, C.M., Yuan, X.L., Xiao, S.H., Chen, Z. and Hua, H. 2019. Ediacaran integrative stratigraphy and timescale of China. *Science China Earth Sciences*, **62**, 7–24, <https://doi.org/10.1007/s11430-017-9216-2>
- Zhou, D. and Graham, S. 1996. The Songpan–Ganzi complex of the West Qinling Shan as a Triassic remnant ocean basin. *In: Yin, A. and Harrison, T.M. (eds) The Tectonic Evolution of Asia*. Cambridge University Press, New York, 281–299.